Discrete moments models for Vlasov equations with non constant strong magnetic limit

Frédérique Charles, Bruno Després, Ruiyang Dai, Sever Adrian Hirstoaga

Discrete moments models for Vlasov equations with non constant strong magnetic limit

F. Charles, B. Després, R. Dai, S. A. Hirstoaga

December 15, 2022

Abstract

We describe the structure of an original application of the method of moments to the Vlasov-Poisson system with non constant strong magnetic field in three dimensions of space. Using basis functions which are aligned with the magnetic field, one obtains a Friedrichs system where the kernel of the singular part is made explicit. A projection of the original model on this kernel yields what we call the reduced model. Basic numerical tests of the field illustrate the accuracy of our implementation. A new generating formula for Laguerre polynomials is obtained in the appendix as a byproduct of the analysis. This study has been supported by ANR MUFFIN ANR-19-CE46-0004.

Abstract

The second author dedicates this work to our late colleague Roland Glowinski.

1 Introduction

We consider a plasma confined by a strong external magnetic field in which electrostatic forces between ions and electrons tend to restore charge equilibrium. As usual in fusion plasma [30], we consider that the time scale of collisions is so large that a collisionless Vlasov equation is enough to describe the dynamics of the particles. For the simplicity of the presentation, we consider that a population of ions moves above a bath of static ions. The population of ions is described with the density function $f(\mathbf{x}, \mathbf{v}, t) \geq 0$ where $\mathbf{x} \in \Omega \subset \mathbb{R}^3$ and $\mathbf{v} \in \mathbb{R}^3$. The model problem for the description of our results is a Vlasov equation with non constant magnetic field

$$\partial_t f + \mathbf{v} \cdot \nabla_x f + \left(\mathbf{E}(\mathbf{x}, t) + \frac{1}{\varepsilon} \mathbf{v} \times \mathbf{B}_0(\mathbf{x}) \right) \cdot \nabla_v f = 0. \tag{1}$$

In this equation $\mathbf{x} \in \mathbb{R}^3$ is the space variable, $\mathbf{v} \in \mathbb{R}^3$ is the velocity variable, $t > 0$ is the time variable and $f = f(\mathbf{x}, \mathbf{v}, t)$ is the unknown. The self-consistent electric field is $\mathbf{E}(\mathbf{x}, t)$ and usually is the solution of a Poisson equation which

expresses the electrical balance of the plasma ions+electrons. For the simplicity, the exterior magnetic field $\mathbf{B}_0(\mathbf{x}) \neq \mathbf{0}$ is constant in time. It is written as

$$\mathbf{B}_0(\mathbf{x}) = \omega(\mathbf{x})\mathbf{b}_0(\mathbf{x}) \tag{2}$$

where $|\mathbf{b}_0(\mathbf{x})| = 1$ and the magnitude of the magnetic field is $\omega(\mathbf{x}) > 0$ (also called the cyclotron frequency). The regime of strong magnetic field in (1) corresponds to the limit $\varepsilon \to 0^+$.

A direct numerical discretization of kinetic equations such as (1) in dimension 3+3 generates a huge computational burden, that is why it is necessary to investigate reduced discrete models. Large magnetic fields usually lead to the so-called drift-kinetic limit [1, 4, 22]. After the seminal development [19] of a specific drift-kinetic model, various justifications have been obtained [7, 21] essentially by considering simplified geometrical configurations. With this respect, the recent reference [14] is a landmark since it considers a general 3-dimensional magnetic field with non constant direction: the limit model is a gyrokinetic model in dimension 3+2 in the general case. In the case where $\nabla \cdot \mathbf{b}_0 = 0$, it can be written as a series of separate gyrokinetic models in dimension 3+1. The gyrokinetic velocity variables of the 3+2 model are the scalar parallel velocity $v = \mathbf{v} \cdot \mathbf{b}_0$ and the square of the modulus of the perpendicular velocity $w = \frac{|\mathbf{v}-v\mathbf{b}_0|^2}{2} = \frac{|\mathbf{v}_\perp|^2}{2}$. There is only one gyrokinetic variable v for the 3+1 model. In the physical community, gyrokinetic models are usually considered as the main avenue for numerical simulations of such complex flows [4, 24, 3, 26, 20]. Mathematically justified gyrokinetics models can be found in [15, 16, 19, 32].

The aim of this work is to describe a new method which can be used to construct reduced numerical models in the limit of non constant strong magnetic fields. It is based on the methods of moments [26, 23, 8, 9, 27, 35] which is currently investigated with original results in [11, 12, 13]. Usually the method of moments is used in a fixed frame because it is amenable to the exact calculation of the numerical coefficients of the method. A natural question is to extend the method of moments to non constant frames which are characteristics of the geometry of fusion devices such as Tokamaks [30, 36, 20, 26, 22, 3, 4]. To the best of our knowledge, it is the first time that the method of moments is studied in dimension 3+3 with **non constant** magnetic field.

The mathematical form of our moment model which approximates (1) writes as

$$\partial_t U + \sum_{i=1}^{3} \partial_{x_i} \left(A_i(\mathbf{x})U \right) - B(\mathbf{x})U + \sum_{i=1}^{3} E_i(\mathbf{x},t)D_i(\mathbf{x})U = \frac{1}{\varepsilon}C(\mathbf{x})U \tag{3}$$

where $U(\mathbf{x},t)$ is a finite vector of moments $\int f(\mathbf{x},\mathbf{v},t)\varphi_i(\mathbf{v})dv$ with respect to a certain orthonormal family of basis functions in the velocity variable $\varphi_i(\mathbf{v},\mathbf{x})$, the transport matrices $A_i(\mathbf{x})_{1 \leq i \leq 3}$ and $B(\mathbf{x})$ represent the action of the operator $\mathbf{v} \cdot \nabla_x$, the matrix $\sum_{i=1}^{3} E_i(\mathbf{x},t)D_i(\mathbf{x})$ represents the action of the operator $\mathbf{E}(\mathbf{x},t) \cdot \nabla_v$. The last matrix $C(\mathbf{x})$ is the numerical realization of the operator $-\mathbf{v} \times \mathbf{B}_0 \cdot \nabla_v$. Note that this term is written for convenience on the right hand

2

side in order to make visible that it acts as a stiff term in the regime $\varepsilon \to 0^+$. In our case we use moments with respect to the Hermite basis which is adapted to Maxwellian profiles [35]. All matrices are explicitly computable and sparse. The numerical cost of a model (3) is proportional to the number of moments. If one desires to use all polynomials in $\mathbf{v} = (v_1, v_2, v_3)$ up to a certain total degree N, then the number of moments is $\text{size}(U) = \text{Card}\{\varphi_i\}$. An elementary counting argument shows that

$$\text{size}(U) = \text{Card}\{(n_1, n_2, n_3) \in \mathbb{N}^3, n_1+n_2+n_3 \le N\} = \frac{(N+1)(N+2)(N+3)}{6}.$$

Our original results are based on the fact that one can adapt the basis functions locally with respect to the magnetic direction $\mathbf{b}_0$. This is the reason why the basis functions $\varphi_i(\mathbf{x}, \mathbf{v})$ are anisotropic. The main property is that the kernel of the matrix C is explicit and independent of $\mathbf{x}$, because the basis functions are in some sense aligned with the magnetic field. Then one can pass, at least formally, to the limit $\varepsilon \to 0^+$. One obtains a simplified Friedrichs system

$$\partial_t \widetilde{U} + \sum_{i=1}^{3} \partial_{x_i} \left(\widetilde{A}_i(\mathbf{x})\widetilde{U} \right) - \widetilde{B}(\mathbf{x})\widetilde{U} + \sum_{i=1}^{3} E_i(\mathbf{x})\widetilde{D}_i(\mathbf{x})\widetilde{U} = 0. \tag{4}$$

The results are formalized in Proposition 4.3. The gains with respect to (3) are twofold. Firstly, the singular term $O(\varepsilon^{-1})$ is no more present. Secondly, the size of the unknown vector is reduced since

$$\text{size}(\widetilde{U}) = \text{Card}\{(m_0, s) \in \mathbb{N}^2, m_0 + 2s \le N\} = \begin{cases} \frac{(N+1)(N+3)}{4}, & N \text{ odd}, \\ \frac{(N+1)(N+3)+1}{4}, & N \text{ even}. \end{cases} \tag{5}$$

So obviously $\text{size}(\widetilde{U}) \ll \text{size}(U)$ for large value of N, which results in a reduction of the number of unknowns in the limit of strong magnetic field.

The organization of the work is as follows. Section 2 deals with the presentation of the method of moments adapted to anisotropic non constant magnetic field. For the simplicity of the presentation this is explained with a electric field $\mathbf{E} \equiv 0$ but it is not a restriction. In Section 3 we analyze the kernel of the matrix C and show the fundamental property which is that is independent of the space variable. It allows to write the reduced moment model (4) which is the main contribution of this work. Then, we show how to reintroduce a self consistent electric field $\mathbf{E} \not\equiv 0$ in Section 4. The final Section 5 is dedicated to numerical illustrations with basic test problems of the field.

2 Construction of the method of moments

We present the main idea of the method of moments applied to the simplified Vlasov equation $\partial_t f + \mathbf{v} \cdot \nabla_x f + \frac{1}{\varepsilon}\mathbf{v} \times \mathbf{B}_0(\mathbf{x}) \cdot \nabla_v f = 0$, where the electric field is discarded for the simplicity of the presentation. We start from basic material about Hermite functions, then present the variational form of the model and finally realize the moment model as a Friedrichs system.

3

2.1 Hermite functions

The Hermite functions are denoted as $\varphi_n(v) = (2^n n! \sqrt{\pi})^{-\frac{1}{2}} e^{\frac{-v^2}{2}} H_n(v)$ for $n \in \mathbb{N}$ where $(H_n)_{n \in \mathbb{N}}$ is the family of Hermite polynomials [31]. A generating formula is

$$\varphi_n(v) = (-1)^n (2^n n! \sqrt{\pi})^{-\frac{1}{2}} e^{\frac{v^2}{2}} \frac{d^n}{dv^n} e^{-v^2}. \tag{6}$$

The first terms in the series are

$$\varphi_0(v) = \pi^{-\frac{1}{4}} e^{-\frac{v^2}{2}}, \ \ \varphi_1(v) = \sqrt{2} \pi^{-\frac{1}{4}} v e^{-\frac{v^2}{2}}, \ \ \varphi_2(v) = \left(\sqrt{2} \pi^{\frac{1}{4}} \right)^{-1} (2v^2 - 1) e^{-\frac{v^2}{2}}. \tag{7}$$

The Hermite functions form an orthonormal family $\int_{\mathbb{R}} \varphi_m(v) \varphi_n(v) dv = \delta_{mn}$ which is complete in the space of quadratically integrable functions $L^2(\mathbb{R})$. For all g such that $\int_{\mathbb{R}} g^2(v) dv < \infty$, one has the identity in $L^2(\mathbb{R})$

$$g(v) = \sum_{n \in \mathbb{N}} g_n \varphi_n(v) dv \qquad \text{where } g_n = \int_{\mathbb{R}} \varphi_n(v) g(v) dv.$$

Two important formulas are

$$v \varphi_n(v) = \sqrt{\frac{n+1}{2}} \varphi_{n+1}(v) + \sqrt{\frac{n}{2}} \varphi_{n-1}(v), \quad n \in \mathbb{N}, \tag{8}$$

and

$$\varphi_n'(v) = -\sqrt{\frac{n+1}{2}} \varphi_{n+1}(v) + \sqrt{\frac{n}{2}} \varphi_{n-1}(v), \quad n \in \mathbb{N}, \tag{9}$$

As in [8, 23], it is convenient to define the asymmetric functions

$$\psi_n(v) = e^{-\frac{v^2}{2}} \varphi_n(v) = (2^n n! \sqrt{\pi})^{-\frac{1}{2}} e^{-v^2} H_n(v),$$
$$\psi^n(v) = e^{\frac{v^2}{2}} \varphi_n(v) = (2^n n! \sqrt{\pi})^{-\frac{1}{2}} H_n(v).$$

Lemma 2.1. *One has the identities* $(\psi_n)'(v) = -\sqrt{2(n+1)} \ \psi_{n+1}(v)$ *and* $(\psi^n)'(v) = \sqrt{2n} \ \psi^{n-1}(v)$ *for* $n \geq 0$.

Proof. The property is a rephrasing of the fact that Hermite polynomials form an Appel's sequence. From (8-9) one obtains

$$\frac{d}{dv} \left(e^{\frac{-v^2}{2}} \varphi_n(v) \right) = e^{\frac{-v^2}{2}} (\varphi_n'(v) - v \varphi_n(v)) = e^{\frac{-v^2}{2}} \left(-\sqrt{2(n+1)} \ \varphi_{n+1}(v) \right)$$

which is the first part of the claim. The second part comes from $\frac{d}{dv} \left(e^{\frac{v^2}{2}} \varphi^n(v) \right) = e^{\frac{v^2}{2}} (\varphi_n'(v) + v \varphi_n(v)) = e^{\frac{v^2}{2}} \left(\sqrt{2n} \ \varphi_{n-1}(v) \right).$ $\qquad \square$

4

2.2 Anisotropic basis functions

Multidimensional basis functions are obtained with anisotropic tensorization of the Hermite functions. A generic notation for a multi-index with three components is

$$\mathbf{n} = (n_0, n_1, n_2) \in \mathbb{N}^3 \text{ with } |\mathbf{n}| = n_0 + n_1 + n_2.$$

We complete $\mathbf{b}_0(\mathbf{x})$ as a local direct orthonormal basis $(\mathbf{b}_0(\mathbf{x}), \mathbf{b}_1(\mathbf{x}), \mathbf{b}_2(\mathbf{x}))$ that is $\mathbf{b}_i(\mathbf{x}) \cdot \mathbf{b}_j(\mathbf{x}) = \delta_{ij}$. To be compatible with physical sound Maxwellian profiles [8], we rescale the directions

$$\mathbf{d}_i(\mathbf{x}) = \frac{\mathbf{b}_i(\mathbf{x})}{\sqrt{T}}, \qquad i = 1, 2, \tag{10}$$

where $\mathbf{b}_0$ is defined in (2) and $T > 0$ is a given reference temperature, assumed to be constant in space and time in this simple modeling. We define

$$\boldsymbol{\varphi}_{\mathbf{n}}(\mathbf{x}, \mathbf{v}) = \varphi_{n_0}\left(\mathbf{v} \cdot \mathbf{d}_0(\mathbf{x})\right) \varphi_{n_1}\left(\mathbf{v} \cdot \mathbf{d}_1(\mathbf{x})\right) \varphi_{n_2}\left(\mathbf{v} \cdot \mathbf{d}_2(\mathbf{x})\right), \tag{11}$$

which is an orthogonal and complete family with respect to the velocity variable $\mathbf{v}$, with continuous dependance with respect to the space variable $\mathbf{x}$. The corresponding asymmetric functions are defined as

$$\boldsymbol{\psi}_{\mathbf{n}}(\mathbf{x}, \mathbf{v}) = \psi_{n_0}\left(\mathbf{v} \cdot \mathbf{d}_0(\mathbf{x})\right) \psi_{n_1}\left(\mathbf{v} \cdot \mathbf{d}_1(\mathbf{x})\right) \psi_{n_2}\left(\mathbf{v} \cdot \mathbf{d}_2(\mathbf{x})\right) \tag{12}$$

and

$$\boldsymbol{\psi}^{\mathbf{n}}(\mathbf{x}, \mathbf{v}) = \psi^{n_0}\left(\mathbf{v} \cdot \mathbf{d}_0(\mathbf{x})\right) \psi^{n_1}\left(\mathbf{v} \cdot \mathbf{d}_1(\mathbf{x})\right) \psi^{n_2}\left(\mathbf{v} \cdot \mathbf{d}_2(\mathbf{x})\right) \tag{13}$$

By construction

$$\boldsymbol{\psi}_{\mathbf{n}}(\mathbf{x}, \mathbf{v}) = e^{-\frac{|\mathbf{v}|^2}{2T}} \boldsymbol{\varphi}_{\mathbf{n}}(\mathbf{x}, \mathbf{v}) \text{ and } \boldsymbol{\psi}^{\mathbf{n}}(\mathbf{x}, \mathbf{v}) = e^{\frac{|\mathbf{v}|^2}{2T}} \boldsymbol{\varphi}_{\mathbf{n}}(\mathbf{x}, \mathbf{v}). \tag{14}$$

For further technical convenience we define the matrix

$$M(\mathbf{x}) = (m_{ij}(\mathbf{x}))_{1 \le i, j \le 3} = (\mathbf{b}_0(\mathbf{x}) \mid \mathbf{b}_1(\mathbf{x}) \mid \mathbf{b}_2(\mathbf{x}))$$

which is orthonormal $M^t M = I$. We will consider the local change of variable $\mathbf{v} \mapsto \mathbf{w} = (\mathbf{v} \cdot \mathbf{d}_0(\mathbf{x}), \mathbf{v} \cdot \mathbf{d}_1(\mathbf{x}), \mathbf{v} \cdot \mathbf{d}_2(\mathbf{x}))^t = \frac{1}{\sqrt{T}} M^t(\mathbf{x}) \mathbf{v}$. One note that

$$\mathbf{v} = T^{\frac{1}{2}} M(\mathbf{x}) \mathbf{w} \text{ and } dv = T^{\frac{3}{2}} dw. \tag{15}$$

2.3 Weak form of the moment model

With the previous notations, the variational form of the method of moments is based on a finite expansion formula which is then plugged in the weak form. It writes as

$$\begin{aligned} f^N(\mathbf{x}, \mathbf{v}, t) &= \sum_{|\mathbf{m}| \le N} u_{\mathbf{m}}(\mathbf{x}, t) \boldsymbol{\psi}_{\mathbf{m}}(\mathbf{x}, \mathbf{v}), \\ \int g^N(\mathbf{x}, \mathbf{v}, t) \boldsymbol{\psi}^{\mathbf{n}}(\mathbf{x}, \mathbf{v}) dv &= 0 \quad \text{for } |\mathbf{n}| \le N, \end{aligned} \tag{16}$$

where

$$g^N(\mathbf{x}, \mathbf{v}, t) = \partial_t f^N(\mathbf{x}, \mathbf{v}, t) + \mathbf{v} \cdot \nabla_x f^N(\mathbf{x}, \mathbf{v}, t) + \frac{1}{\varepsilon} \mathbf{v} \times \mathbf{B}_0(\mathbf{x}) \cdot \nabla_v f^N(\mathbf{x}, \mathbf{v}, t).$$

The moments are the functions $u_{\mathbf{m}}(\mathbf{x}, t)$. Their number is $\frac{(N+1)(N+2)(N+3)}{6}$.

2.4 Matrix form of the moment model

The transport matrices allow to rewrite the equations (16) for the unknown vector $U(\mathbf{x}, t) = (u_{\mathbf{m}}(\mathbf{x}, t))_{|\mathbf{m}| \leq N}$ The transport matrices in space are $A_i(\mathbf{x}) = \left(a_{\mathbf{nm}}^i(\mathbf{x}) \right)_{|\mathbf{m}|, |\mathbf{n}| \leq N}$ with

$$a_{\mathbf{nm}}^i(\mathbf{x}) = \int_{\mathbf{v}} \boldsymbol{\psi}_{\mathbf{m}}(\mathbf{x}, \mathbf{v}) \boldsymbol{\psi}^{\mathbf{n}}(\mathbf{x}, \mathbf{v}) v_i dv, \qquad i = 1, 2, 3.$$

A related matrix is $B(\mathbf{x}) = (b_{\mathbf{nm}}(\mathbf{x}))_{|\mathbf{m}|, |\mathbf{n}| \leq N}$ with

$$b_{\mathbf{nm}}(\mathbf{x}) = \int_{\mathbf{v}} \boldsymbol{\psi}_{\mathbf{m}}(\mathbf{x}, \mathbf{v}) \mathbf{v} \cdot \nabla_x \boldsymbol{\psi}^{\mathbf{n}}(\mathbf{x}, \mathbf{v}) dv.$$

Note that if the bulk magnetic field $\mathbf{B}_0$ is constant in space, then the anisotropic basis functions can naturally be taken independent of the space variable. Then $B = 0$ as well. The transport matrice in velocity is $C(\mathbf{x}) = (c_{\mathbf{nm}}(\mathbf{x}))_{|\mathbf{m}|, |\mathbf{n}| \leq N}$ with

$$c_{\mathbf{mn}}(\mathbf{x}) = \int_{\mathbf{v}} \boldsymbol{\psi}_{\mathbf{m}}(\mathbf{x}, \mathbf{v}) \mathbf{v} \times \mathbf{B}_0(\mathbf{x}) \cdot \nabla_v \boldsymbol{\psi}^{\mathbf{n}}(\mathbf{x}, \mathbf{v}) dv.$$

Lemma 2.2. *The equations (16) are equivalent to the system*

$$T^{\frac{3}{2}} \partial_t U(\mathbf{x}, t) + \sum_{i=1}^3 \partial_{x_i} (A_i(\mathbf{x}) U(\mathbf{x}, t)) - B(\mathbf{x}) U(\mathbf{x}, t) = \frac{1}{\varepsilon} C(\mathbf{x}) U(\mathbf{x}, t). \quad (17)$$

Proof. Consider the equations (16). Integrals below are written with respect to the velocity variable $\mathbf{v}$ while sums are written with respect to $\mathbf{m}$ such that $|\mathbf{m}| \leq N$. One has for all $|\mathbf{n}| \leq N$

$$\int_{\mathbf{v}} \partial_t f^N \boldsymbol{\psi}^{\mathbf{n}} \quad = T^{\frac{3}{2}} \sum_{\mathbf{m}} \int \boldsymbol{\psi}_{\mathbf{m}} \boldsymbol{\psi}^{\mathbf{n}} dw \ \partial_t u_{\mathbf{m}} \quad = T^{\frac{3}{2}} \partial_t u_{\mathbf{n}}. \quad (18)$$

One also has

$$
\begin{aligned}
\int \left(\mathbf{v} \cdot \nabla_x f^N \right) \boldsymbol{\psi}^{\mathbf{n}} \quad &= \nabla_x \cdot \int \mathbf{v} f^N \boldsymbol{\psi}^{\mathbf{n}} - \int f^N \mathbf{v} \cdot \nabla_x \boldsymbol{\psi}^{\mathbf{n}} \\
&= \sum_{i=1}^3 \partial_{x_i} \sum_{\mathbf{m}} \int v_i \boldsymbol{\psi}_{\mathbf{m}} \boldsymbol{\psi}^{\mathbf{n}} \ u_{\mathbf{m}} - \sum_{\mathbf{m}} \int \boldsymbol{\psi}_{\mathbf{m}} \mathbf{v} \cdot \nabla_x \boldsymbol{\psi}^{\mathbf{n}} \ u_{\mathbf{m}}.
\end{aligned}
\quad (19)
$$

One finally has that

$$
\begin{aligned}
\int \left(\mathbf{v} \times \mathbf{B}_0(\mathbf{x}) \cdot \nabla_v f^N \right) \boldsymbol{\psi}^{\mathbf{n}} \quad &= \int \mathbf{v} \times \mathbf{B}_0(\mathbf{x}) \cdot \nabla_v (f^N \boldsymbol{\psi}^{\mathbf{n}}) \\
&\quad - \int f^N \mathbf{v} \times \mathbf{B}_0(\mathbf{x}) \cdot \nabla_v \boldsymbol{\psi}^{\mathbf{n}} \\
&= - \int f^N \mathbf{v} \times \mathbf{B}_0(\mathbf{x}) \cdot \nabla_v \boldsymbol{\psi}^{\mathbf{n}} \\
&= - \sum_{\mathbf{m}} \int \boldsymbol{\psi}_{\mathbf{m}} \mathbf{v} \times \mathbf{B}_0(\mathbf{x}) \cdot \nabla_v \boldsymbol{\psi}^{\mathbf{n}} \ u_{\mathbf{m}}
\end{aligned}
\quad (20)
$$

The summation of (18-20) yields the line that corresponds to the index $\mathbf{n}$ in (17), with the difference that the terms with a minus sign (19-20) correspond to the matrices B and C with a plus sign in the right hand side of the claim. $\square$

The transport matrices A_1, A_2 and A_3 and the source matrices B and C satisfy some properties which are explicitly given below.

Lemma 2.3. *The transport matrices A_1, A_2 and A_3 are symmetric.*

Proof. By definition of the asymmetric basis $\boldsymbol{\psi^m}$ and $\boldsymbol{\psi_n}$, one has

$$a_{\mathbf{n,m}}^i = \int_{\mathbf{v}} \boldsymbol{\varphi_m}(\mathbf{x,v})\boldsymbol{\varphi_n}(\mathbf{x,v})v_i dv = \int_{\mathbf{v}} \boldsymbol{\varphi_n}(\mathbf{x,v})\boldsymbol{\varphi_m}(\mathbf{x,v})v_i dv = a_{\mathbf{m,n}}^i$$

which establishes the symmetry property of A^i. $\qquad\square$

Lemma 2.4. *One has $\sum_{i=1}^{3} \partial_{x_i} A^i(\mathbf{x}) = B(\mathbf{x}) + B^t(\mathbf{x})$.*

Proof. On the one hand $\sum_{i=1}^{3} \partial_{x_i} a_{\mathbf{n,m}}^i = \int \mathbf{v} \cdot \nabla_x \boldsymbol{\psi_m}\boldsymbol{\psi^n} + \int \boldsymbol{\psi_m}\mathbf{v} \cdot \nabla_x \boldsymbol{\psi^n}$. On the other hand one obtains

$$
\begin{aligned}
b_{\mathbf{n,m}} + b_{\mathbf{m,n}} \quad &= \int \boldsymbol{\psi_m}\mathbf{v} \cdot \nabla_x \boldsymbol{\psi^n} + \int \boldsymbol{\psi_n}\mathbf{v} \cdot \nabla_x \boldsymbol{\psi^m} \\
&= \int \boldsymbol{\psi_m}\mathbf{v} \cdot \nabla_x \boldsymbol{\psi^n} + \int \boldsymbol{\psi_n}\mathbf{v} \cdot \nabla_x \left(e^{\frac{|\mathbf{v}|^2}{T}} \boldsymbol{\psi_m} \right) \\
&= \int \boldsymbol{\psi_m}\mathbf{v} \cdot \nabla_x \boldsymbol{\psi^n} + \int \boldsymbol{\psi^n}\mathbf{v} \cdot \nabla_x \boldsymbol{\psi_m} \\
&= \sum_{=1}^{3} \partial_{x_i} a_{\mathbf{n,m}}^i
\end{aligned}
$$

which is the claim. $\qquad\square$

Lemma 2.5. *The matrix C is antisymmetric.*

Proof. Indeed one has

$$
\begin{aligned}
c_{\mathbf{n,m}} + c_{\mathbf{m,n}} \quad &= \int \boldsymbol{\psi_m}\mathbf{v} \times \mathbf{B}_0 \cdot \nabla_v \boldsymbol{\psi^n} + \int \boldsymbol{\psi_n}\mathbf{v} \times \mathbf{B}_0 \cdot \nabla_v \boldsymbol{\psi^m} \\
&= \int \boldsymbol{\psi_m}\mathbf{v} \times \mathbf{B}_0 \cdot \nabla_v \boldsymbol{\psi^n} + \int \boldsymbol{\psi_n}\mathbf{v} \times \mathbf{B}_0 \cdot \nabla_v \left(e^{\frac{|\mathbf{v}|^2}{T}} \boldsymbol{\psi_m} \right) \\
&= \int \boldsymbol{\psi_m}\mathbf{v} \times \mathbf{B}_0 \cdot \nabla_v \boldsymbol{\psi^n} + \int \boldsymbol{\psi^n}\mathbf{v} \times \mathbf{B}_0 \cdot \nabla_v \boldsymbol{\psi_m}
\end{aligned}
$$

because $\mathbf{v} \times \mathbf{B}_0 \cdot \nabla_v e^{\frac{|\mathbf{v}|^2}{T}} = 0$. Therefore

$$
\begin{aligned}
c_{\mathbf{n,m}} + c_{\mathbf{m,n}} \quad &= \int \boldsymbol{\psi_m}\mathbf{v} \times \mathbf{B}_0 \cdot \nabla_v \boldsymbol{\psi^n} + \int \boldsymbol{\psi^n}\mathbf{v} \times \mathbf{B}_0 \cdot \nabla_v \boldsymbol{\psi_m} \\
&= \int \boldsymbol{\psi_m}\mathbf{v} \times \mathbf{B}_0 \cdot \nabla_v \boldsymbol{\psi^n} + \int \mathbf{v} \times \mathbf{B}_0 \cdot \nabla_v \boldsymbol{\psi_m} \int \boldsymbol{\psi^n} \\
&= \int \nabla_v \cdot (\mathbf{v} \times \mathbf{B}_0 \boldsymbol{\psi_m}\boldsymbol{\psi^n}) = 0
\end{aligned}
$$

which is the claim. $\qquad\square$

These properties already guarantee the quadratic stability of the moment model which has the form of a Friedrichs system.

Lemma 2.6. *One has $T^{\frac{3}{2}}\partial_t |U|^2(\mathbf{x},t) + \sum_{i=1}^{3} \partial_{x_i} (A_i U \cdot U)(\mathbf{x},t) = 0$.*

Proof. This is classical Friedrichs systems but we give the proof because it is an important property of the model. Taking the scalar product of (17) against $2U$ and using the antisymmetry of C, one gets $T^{\frac{3}{2}}\partial_t |U|^2 + 2\sum_{i=1}^{3} (\partial_{x_i} A_i U) \cdot U = 2BU \cdot U = (B + B^t)U \cdot U$. That is

$$T^{\frac{3}{2}}\partial_t |U|^2 + 2\sum_{i=1}^{3} (\partial_{x_i} A_i) U \cdot U + 2\sum_{i=1}^{3} A_i (\partial_{x_i} U) \cdot U = \sum_{i=1}^{3} (\partial_{x_i} A_i) U \cdot U.$$

Simplification and the symmetry of the A_i yields

$$T^{\frac{3}{2}}\partial_t|U|^2 + \sum_{i=1}^{3}(\partial_{x_i}A_i)\,U\cdot U + \sum_{i=1}^{3}A_i\,(\partial_{x_i}U)\cdot U + \sum_{i=1}^{3}A_iU\cdot(\partial_{x_i}U) = 0.$$

Recombination yields the claim. $\qquad\square$

Lemma 2.7. *Assume $N \geq 2$. Solutions to (17) preserve mass and energy.*

Proof. We use the formulation (16) which is equivalent to (17). Considering (7) and (14), (16) yields

$$\int\left(\partial_t f^N + \mathbf{v}\cdot\nabla_x f^N + \mathbf{v}\times\mathbf{B}_0\cdot\nabla_v f^N\right)\psi\,dv = 0 \qquad (21)$$

for all ψ which can be obtained by linear combination of the $\psi^{\mathbf{n}}$ for $|\mathbf{n}| \leq N$. For $\psi = \pi^{\frac{3}{4}}\psi^{\mathbf{0}} = 1$, one gets the equation of conservation of mass $\partial_t\int f^N dv + \nabla_x\cdot\int f^N\mathbf{v}dv = 0$. Now let us take another test function

$$\psi^{(0,0,0)} = \pi^{\frac{3}{4}}T\left(\frac{1}{\sqrt{2}}\psi^{(2,0,0)} + \frac{1}{\sqrt{2}}\psi^{(0,2,0)} + \frac{1}{\sqrt{2}}\psi^{(0,0,2)} + \frac{3}{2}\psi^{\mathbf{0}}\right),$$

which, by using (7), is exactly the square of the velocity $\psi^{(0,0,0)} = |\mathbf{v}|^2$. One obtains $\partial_t\int f^N|\mathbf{v}|^2 dv + \nabla_x\cdot\int f^N\mathbf{v}|\mathbf{v}|^2 dv + \int\mathbf{v}\times\mathbf{B}_0\cdot\nabla_v f^N|\mathbf{v}|^2 = 0$. The third integral vanishes identically since

$$\int\mathbf{v}\times\mathbf{B}_0\cdot\nabla_v f^N|\mathbf{v}|^2 = \int\nabla_v\cdot\left(\mathbf{v}\times\mathbf{B}_0 f^N\right)|\mathbf{v}|^2 = -\int\left(\mathbf{v}\times\mathbf{B}_0 f^N\right)\cdot\mathbf{v} = 0.$$

It yields the claim. $\qquad\square$

Lemma 2.8. *The transport matrices A_1, A_2 and A_3 and the matrices B and C can be calculated explicitly and are sparse.*

Proof. We explain in detail the formulas firstly for the transport matrix A_1. We consider $a^1_{\mathbf{nm}}(\mathbf{x}) = \int\psi_{\mathbf{m}}(\mathbf{x},\mathbf{v})\psi^{\mathbf{n}}(\mathbf{x},\mathbf{v})v_1 dv = \int\varphi_{\mathbf{m}}(\mathbf{x},\mathbf{v})\varphi_{\mathbf{n}}(\mathbf{x},\mathbf{v})v_1 dv$ and make a local change of variable.

With the notation (15), one has $v_1 = T^{\frac{1}{2}}(m_{11}(\mathbf{x})w_1 + m_{12}(\mathbf{x})w_2 + m_{13}(\mathbf{x})w_3)$, and therefore

$$\begin{aligned}
a^1_{\mathbf{mn}}(\mathbf{x}) \quad = T^2\int \quad & \psi_{m_0}(w_1)\psi_{m_1}(w_2)\psi_{m_2}(w_3)\\
\times \quad & \psi^{n_0}(w_1)\psi^{n_1}(w_2)\psi^{n_2}(w_3)\\
\times \quad & (m_{11}(\mathbf{x})w_1 + m_{12}(\mathbf{x})w_2 + m_{13}(\mathbf{x})w_3)\,dw.
\end{aligned}$$

With separation of variables and the formula (8), one obtains

$$\begin{aligned}
a^1_{\mathbf{nm}}(\mathbf{x}) \quad = \quad & \frac{T^2}{\sqrt{2}}m_{11}(\mathbf{x})\left(\sqrt{m_0+1}\delta_{m_0+1,n_0} + \sqrt{m_0}\delta_{m_0-1,n_0}\right)\delta_{m_1,n_1}\delta_{m_2,n_2}\\
+ \quad & \frac{T^2}{\sqrt{2}}m_{12}(\mathbf{x})\delta_{m_0,n_0}\left(\sqrt{m_1+1}\delta_{m_1+1,n_1} + \sqrt{m_1}\delta_{m_1-1,n_1}\right)\delta_{m_2,n_2}\\
+ \quad & \frac{T^2}{\sqrt{2}}m_{13}(\mathbf{x})\delta_{m_0,n_0}\delta_{m_1,n_1}\left(\sqrt{m_2+1}\delta_{m_2+1,n_2} + \sqrt{m_2}\delta_{m_2-1,n_2}\right).
\end{aligned}$$
$$(22)$$

These formulas show that most of the coefficients vanish. This matrix is sparse. The same method yields

$$
\begin{aligned}
a^2_{\mathbf{nm}}(\mathbf{x}) &= \frac{T^2}{\sqrt{2}} m_{21}(\mathbf{x}) \left(\sqrt{m_0+1}\delta_{m_0+1,n_0} + \sqrt{m_0}\delta_{m_0-1,n_0}\right) \delta_{m_1,n_1}\delta_{m_2,n_2} \\
&+ \frac{T^2}{\sqrt{2}} m_{22}(\mathbf{x})\delta_{m_0,n_0} \left(\sqrt{m_1+1}\delta_{m_1+1,n_1} + \sqrt{m_1}\delta_{m_1-1,n_1}\right) \delta_{m_2,n_2} \\
&+ \frac{T^2}{\sqrt{2}} m_{23}(\mathbf{x})\delta_{m_0,n_0}\delta_{m_1,n_1} \left(\sqrt{m_2+1}\delta_{m_2+1,n_2} + \sqrt{m_2}\delta_{m_2-1,n_2}\right)
\end{aligned}
\tag{23}
$$

and

$$
\begin{aligned}
a^3_{\mathbf{nm}}(\mathbf{x}) &= \frac{T^2}{\sqrt{2}} m_{31}(\mathbf{x}) \left(\sqrt{m_0+1}\delta_{m_0+1,n_0} + \sqrt{m_0}\delta_{m_0-1,n_0}\right) \delta_{m_1,n_1}\delta_{m_2,n_2} \\
&+ \frac{T^2}{\sqrt{2}} m_{32}(\mathbf{x})\delta_{m_0,n_0} \left(\sqrt{m_1+1}\delta_{m_1+1,n_1} + \sqrt{m_1}\delta_{m_1-1,n_1}\right) \delta_{m_2,n_2} \\
&+ \frac{T^2}{\sqrt{2}} m_{33}(\mathbf{x})\delta_{m_0,n_0}\delta_{m_1,n_1} \left(\sqrt{m_2+1}\delta_{m_2+1,n_2} + \sqrt{m_2}\delta_{m_2-1,n_2}\right).
\end{aligned}
\tag{24}
$$

Now consider the coefficients of the matrix $B(\mathbf{x})$ which are written as

$$
b_{\mathbf{mn}}(\mathbf{x}) = \int \boldsymbol{\varphi}_{\mathbf{m}}(\mathbf{x},\mathbf{v})\mathbf{v}\cdot\nabla_x\boldsymbol{\varphi}_{\mathbf{n}}(\mathbf{x},\mathbf{v})dv.
$$

One has

$$
\begin{aligned}
b_{\mathbf{nm}}(\mathbf{x}) &= \int \boldsymbol{\varphi}_{\mathbf{m}}(\mathbf{x},\mathbf{v}) \left(\nabla d_0(\mathbf{x}) : \mathbf{v}\otimes\mathbf{v}\right) \varphi'_{n_0}(w_1)\varphi_{n_1}(w_2)\varphi_{n_2}(w_3)dv \\
&+ \int \boldsymbol{\varphi}_{\mathbf{m}}(\mathbf{x},\mathbf{v}) \left(\nabla d_1(\mathbf{x}) : \mathbf{v}\otimes\mathbf{v}\right) \varphi_{n_0}(w_1)\varphi'_{n_1}(w_2)\varphi_{n_2}(w_3)dv \\
&+ \int \boldsymbol{\varphi}_{\mathbf{m}}(\mathbf{x},\mathbf{v}) \left(\nabla d_2(\mathbf{x}) : \mathbf{v}\otimes\mathbf{v}\right) \varphi_{n_0}(w_1)\varphi_{n_1}(w_2)\varphi'_{n_2}(w_3)dv.
\end{aligned}
$$

Defining $M_i(\mathbf{x}) = M(\mathbf{x})^t\nabla b_i(\mathbf{x})M(\mathbf{x})$ for $i=0,1,2$, one can write

$$
\begin{aligned}
b_{\mathbf{nm}}(\mathbf{x}) &= T^2 M_0(x) : \int \boldsymbol{\varphi}_{\mathbf{m}}(\mathbf{x},\mathbf{v})\mathbf{w}\otimes\mathbf{w}\varphi'_{n_0}(w_1)\varphi_{n_1}(w_2)\varphi_{n_2}(w_3)dw \\
&+ T^2 M_1(x) : \int \boldsymbol{\varphi}_{\mathbf{m}}(\mathbf{x},\mathbf{v})\mathbf{w}\otimes\mathbf{w}\varphi_{n_0}(w_1)\varphi'_{n_1}(w_2)\varphi_{n_2}(w_3)dw \qquad (25) \\
&+ T^2 M_2(x) : \int \boldsymbol{\varphi}_{\mathbf{m}}(\mathbf{x},\mathbf{v})\mathbf{w}\otimes\mathbf{w}\varphi_{n_0}(w_1)\varphi_{n_1}(w_2)\varphi'_{n_2}(w_3)dw.
\end{aligned}
$$

Exact calculation of the integrals is now possible with the formulas (8-9) and the orthonormality of the Hermite functions. Consider finally the coefficients of the matrix C written as

$$
c_{\mathbf{nm}}(\mathbf{x}) = \int_{\mathbf{v}} \boldsymbol{\varphi}_{\mathbf{m}}(\mathbf{x},\mathbf{v})\mathbf{v}\times\mathbf{B}_0(\mathbf{x})\cdot\nabla_v\boldsymbol{\varphi}_{\mathbf{n}}(\mathbf{x},\mathbf{v})dv.
\tag{26}
$$

One has

$$
\begin{aligned}
c_{\mathbf{nm}}(\mathbf{x}) &= \int \boldsymbol{\varphi}_{\mathbf{m}}(\mathbf{x},\mathbf{v}) \left(\mathbf{v}\times\mathbf{B}_0(\mathbf{x})\cdot\mathbf{d}_0(\mathbf{x})\right) \varphi'_{n_0}(w_1)\varphi_{n_1}(w_2)\varphi_{n_2}(w_3)dv \\
&+ \int \boldsymbol{\varphi}_{\mathbf{m}}(\mathbf{x},\mathbf{v}) \left(\mathbf{v}\times\mathbf{B}_0(\mathbf{x})\cdot\mathbf{d}_1(\mathbf{x})\right) \varphi_{n_0}(w_1)\varphi'_{n_1}(w_2)\varphi_{n_2}(w_3)dv \\
&+ \int \boldsymbol{\varphi}_{\mathbf{m}}(\mathbf{x},\mathbf{v}) \left(\mathbf{v}\times\mathbf{B}_0(\mathbf{x})\cdot\mathbf{d}_2(\mathbf{x})\right) \varphi_{n_0}(w_1)\varphi_{n_1}(w_2)\varphi'_{n_2}(w_3)dv.
\end{aligned}
\tag{27}
$$

Since $\mathbf{d}_0$ is aligned with the magnetic field, one has

$$
\begin{aligned}
\mathbf{v}\times\mathbf{B}_0(\mathbf{x})\cdot\mathbf{d}_0(\mathbf{x}) &= 0, \\
\mathbf{v}\times\mathbf{B}_0(\mathbf{x})\cdot\mathbf{d}_1(\mathbf{x}) &= \omega(\mathbf{x})w_3, \\
\mathbf{v}\times\mathbf{B}_0(\mathbf{x})\cdot\mathbf{d}_2(\mathbf{x}) &= -\omega(\mathbf{x})w_2.
\end{aligned}
$$

One gets

$$
\begin{aligned}
c_{\mathbf{nm}}(\mathbf{x}) &= T^{\frac{3}{2}}\omega(\mathbf{x}) \int \boldsymbol{\varphi}_{\mathbf{m}}(\mathbf{x},\mathbf{v}) w_3 \varphi_{n_0}(w_1)\varphi'_{n_1}(w_2)\varphi_{n_2}(w_3)dw \\
&- T^{\frac{3}{2}}\omega(\mathbf{x}) \int \boldsymbol{\varphi}_{\mathbf{m}}(\mathbf{x},\mathbf{v}) w_2 \varphi_{n_0}(w_1)\varphi_{n_1}(w_2)\varphi'_{n_2}(w_3)dw.
\end{aligned}
\tag{28}
$$

Once again, exact calculation of the integrals is possible with the formulas (8-9) and the orthonormality of the Hermite functions. An additional interesting simplification shows up because one has from (8-9)

$$
w_3\varphi'_{n_1}(w_2)\varphi_{n_2}(w_3) - w_2\varphi_{n_1}(w_2)\varphi'_{n_2}(w_3)
$$

$$
= -\sqrt{(n_1+1)n_2}\varphi_{n_1+1}(w_2)\varphi_{n_2-1}(w_3) + \sqrt{n_1(n_2+1)}\varphi_{n_1-1}(w_2)\varphi_{n_2+1}(w_3).
$$

One gets

$$
\begin{aligned}
c_{\mathbf{nm}}(\mathbf{x}) = T^{\frac{3}{2}}\omega(\mathbf{x})\delta_{m_0,n_0} \Big(&-\sqrt{(n_1+1)n_2}\delta_{m_1,n_1+1}\delta_{m_2,n_2-1} \\
&+\sqrt{n_1(n_2+1)}\delta_{m_1,n_1-1}\delta_{m_2,n_2+1} \quad \Big).
\end{aligned}
\tag{29}
$$

It is worthwhile to notice that C is the product of a constant matrix times the coefficient $T^{\frac{3}{2}}\omega(\mathbf{x})$. The sparsity of all matrices is a consequence of the formulas. $\qquad\square$

3 Reduced moment models

The reduced moment model naturally captures the formal limit of strong magnetic field $\varepsilon \to 0^+$ of (3). To construct the reduced model (4), we firstly analyze the kernel of the matrix C. This kernel is called the cyclotron kernel in the following. Then we use this information to reduce (in a sense that will be made explicit) the Friedrichs system (17).

3.1 The cyclotron kernel

The cyclotron kernel is defined as

$$
\mathcal{K} = \{U \mid C(\mathbf{x})U = 0.\}
$$

With the physical assumption that we made $\mathbf{B}_0(\mathbf{x}) \neq 0$, then $\omega(\mathbf{x}) \neq 0$ in (28). Therefore the kernel $\mathcal{K}$ is independent of the space variable $\mathbf{x}$. The sparsity of the matrix C which is consequence of the formula (29) is particularly useful to obtain simple characterizations. One has that $C(\mathbf{x})U = 0$ is equivalent to $|\mathbf{m}| \leq N$ with:
if $m_1, m_2 \geq 1$ then

$$
-\sqrt{m_1(m_2+1)}u_{m_0,m_1-1,m_2+1} + \sqrt{(m_1+1)m_2}u_{m_0,m_1+1,m_2-1} = 0,
\tag{30}
$$

if $m_1 \geq 1$ and $m_2 = 0$ then

$$
-u_{m_0,m_1-1,1} = 0,
\tag{31}
$$

if if $m_1 = 0$ and $m_2 \geq 1$ then

$$u_{m_0,1,m_2-1} = 0. \tag{32}$$

Therefore one has the characterization of the kernel

$$\mathcal{K} = \left\{ U = (u_{\mathbf{m}})_{|\mathbf{m}| \leq N} \mid \quad |\mathbf{m}| \leq N \text{ with either } (30), (31) \text{ or } (32). \right\}.$$

The structure of the recurrence relations defining the kernel is illustrated in Figure 1. Due to (31-32), all coefficients vanish along the column $m = 1$ and along the line $m_2 = 1$. Then by (30), the nullity of the coefficients along the column $m = 1$ and along the line $m_2 = 1$ is propagated along diagonals, one coefficient among two neighboring ones. Therefore if a diagonal has an even number of terms then all the terms vanish. The other case is when the diagonal has an odd number of coefficients, call it $p = m_1 + m_2 + 1 = 2s + 1$. Then s coefficients vanish along the diagonal, while the other $s + 1$ coefficients are linearly dependent through the linear relations (30).
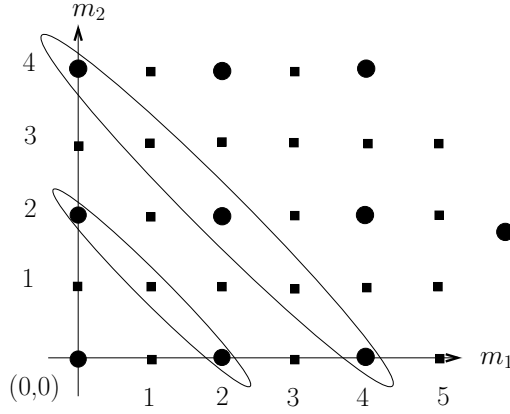

Figure 1: Plot of the coefficients (m_1, m_2), m_0 being given. The squares are vanishing coefficients $\mathbf{u}_{m_0,m_1,m_2} = 0$. The bullets are coefficients which might be non zero $\mathbf{u}_{m_0,m_1,m_2} \neq 0$. The ellipses at 45 degrees indicate that $m_1 + m_2$ is constant along the diagonals.

To make explicit the linear dependence between the remaining non trivial coefficients (the bullets in Figure 1), we concentrate on one non trivial diagonal and set

$$v^{m_0}_{m_1,m_2} = \frac{2^{\frac{m_1}{2}} \left(\frac{m_1}{2}\right)! \, 2^{\frac{m_2}{2}} \left(\frac{m_2}{2}\right)!}{\sqrt{m_1!} \, \sqrt{m_2!}} \mathbf{u}_{m_0,m_1,m_2} \quad \text{where } m_1, m_2 \text{ are even.}$$

Lemma 3.1. *One has* $v^{m_0}_{m_1-1,m_2+1} = v^{m_0}_{m_1+1,m_2-1}$.

Proof. Indeed the kernel relation writes

$$\sqrt{m_1(m_2+1)} \frac{\sqrt{(m_1-1)!}}{2^{\frac{m_1-1}{2}} \left(\frac{m_1-1}{2}\right)!} \frac{\sqrt{(m_2+1)!}}{2^{\frac{m_2+1}{2}} \left(\frac{m_2+1}{2}\right)!} v^{m_0}_{m_1-1,m_2+1}$$

11

$$= \sqrt{(m_1+1)m_2} \frac{\sqrt{(m_1+1)!}}{2^{\frac{m_1+1}{2}}\left(\frac{m_1+1}{2}\right)!} \frac{\sqrt{(m_2-1)!}}{2^{\frac{m_2-1}{2}}\left(\frac{m_2-1}{2}\right)!} v^{m_0}_{m_1+1,m_2-1}$$

which is equivalent to

$$\frac{\sqrt{(m_1)!}}{\left(\frac{m_1-1}{2}\right)!} \frac{(m_2+1)\sqrt{m_2!}}{\left(\frac{m_2+1}{2}\right)!} v^{m_0}_{m_1-1,m_2+1} = \frac{(m_1+1)\sqrt{m_1!}}{\left(\frac{m_1+1}{2}\right)!} \frac{\sqrt{m_2!}}{\left(\frac{m_2-1}{2}\right)!} v^{m_0}_{m_1+1,m_2-1}.$$

Since the coefficients are the same, it ends the proof. $\qquad\square$

3.2 Reduction

The previous formulas have important applications to obtain reduced Friedrichs systems. Let us consider U in the kernel of the matrix C, which is necessarily satisfied by the formal limit $\varepsilon \to 0^+$ of the model (3). Discarding the time variable, we begin explaining the structure of the truncated series

$$f^N(\mathbf{x},\mathbf{v}) = \sum_{|n|\leq N} \mathbf{u_n}\psi_{\mathbf{n}} \qquad \text{where } U = (\mathbf{u_n})_{|\mathbf{n}|\leq N} \in \mathcal{K}.$$

One has

$$f^N(\mathbf{x},\mathbf{v}) = e^{-\frac{|\mathbf{v}|^2}{2T}} \sum_{m_0=0}^{N} \psi_{m_0}(w_1) \left(\sum_{q=0}^{m_0} \sum_{m_1+m_2=q} \mathbf{u}_{m_0,m_1,m_2}\psi_{m_1}(w_2)\psi_{m_2}(w_3) \right).$$

If q is odd, then $\mathbf{u}_{m_0,m_1,m_2} = 0$. If q is even, then $\mathbf{u}_{m_0,m_1,m_2} = 0$ for m_1 and/or m_2 odd. If $q = 2s$ is even, then one can write

$$\mathbf{u}_{m_0,2r,2s-2r} = \frac{\sqrt{(2r)!(2s-2r)!}}{2^s r!(s-r)!} v^{m_0}_q \tag{33}$$

where $v^{m_0}_q$ depends only on the index of the diagonal $q = 2s = m_1 + m_2$. For $q = 2s$, on considers $\sum_{m_1+m_2=q} \mathbf{u}_{m_0,m_1,m_2}\psi_{m_1}(w_2)\psi_{m_2}(w_3) = F_s(w_2,w_3)v^{m_0}_{2s}$ where

$$F_s(w_2,w_3) = \sum_{r=0}^{s} \frac{\sqrt{(2r)!(2s-2r)!}}{2^s r!(s-r)!} \psi_{2r}(w_2)\psi_{2s-2r}(w_3) \text{ and } v^{m_0}_{2s} \in \mathbb{R}.$$

One obtains

$$f^N(\mathbf{x},\mathbf{v}) = e^{-\frac{|\mathbf{v}|^2}{2T}} \sum_{m_0=0}^{N} \psi_{m_0}(w_1) \sum_{s=0}^{\lfloor\frac{N-m_0}{2}\rfloor} F_s(w_2,w_3)v^{m_0}_{2s}.$$

Lemma 3.2 (Proof in the appendix). *Let* $(L_s)_{s\in\mathbb{N}}$ *be the family of Laguerre polynomials. One has*

$$F_s(w_2,w_3) = (-1)^s 4^s s! e^{-\frac{w_2^2+w_3^2}{2}} L_s(w_2^2+w_3^2), \quad s \in \mathbb{N}. \tag{34}$$

12

Plugging this formula in the representation of f^N, one obtains finally

$$f^N(\mathbf{x}, \mathbf{v}) = e^{-|\mathbf{w}|^2} \sum_{m_0=0}^{N} H_{m_0}(w_0) \sum_{s=0}^{\lfloor \frac{N-m_0}{2} \rfloor} L_s(w_2^2 + w_3^2)\alpha_{m_0,s}$$

where the degrees of freedom are some coefficients $\alpha_{m_0,s} \in \mathbb{R}$. One recovers an approximation method based on Hermite-Laguerre polynomials, already known in plasma physics for gyrokinetic model [25, 20, 26, 28].

Next we define the rectangular matrix that corresponds to the transformation (33). We need a generic notation for multi-index with two components

$$\widetilde{\mathbf{n}} = (\widetilde{n}_0, \widetilde{n}_1) \in \mathbb{N}^2 \text{ with } |\widetilde{\mathbf{n}}| = \widetilde{n}_0 + 2\widetilde{n}_1.$$

One an check that the number of moments such that $\widetilde{n}_0 + 2\widetilde{n}_1 \leq N$ is given by formula (5). One defines the rectangular matrix $P = \big(p_{\mathbf{m},\widetilde{\mathbf{n}}}\big)_{|\mathbf{m}|,|\widetilde{\mathbf{n}}| \leq N}$ with

$$p_{\mathbf{m},\widetilde{\mathbf{n}}} = \delta_{m_0,\widetilde{n}_0}\delta_{\mathrm{mod}(m_1,2),0}\delta_{\mathrm{mod}(m_2,2),0}\delta_{m_1+m_2,2\widetilde{n}_1}\frac{\sqrt{(m_1)!(m_2)!}}{2^{\frac{m_1+m_2}{2}}\frac{m_1}{2}!\frac{m_2}{2}!}. \tag{35}$$

Lemma 3.3. $|\mathbf{m}| \neq |\widetilde{\mathbf{n}}| \implies p_{\mathbf{m},\widetilde{\mathbf{n}}} = 0.$

Proof. Indeed if $|\mathbf{m}| \neq |\widetilde{\mathbf{n}}|$, then either $\delta_{m_0,\widetilde{n}_0} = 0$ or $\delta_{m_1+m_2,2\widetilde{n}_1} = 0$. $\qquad \square$

By definition of the matrix P, one has that

$$U = (\mathbf{u_m})_{|\mathbf{m}| \leq N} \in \mathcal{K} \iff U = P\widetilde{U} \text{ for some } U = (\widetilde{\mathbf{u}}_{\widetilde{\mathbf{n}}})_{|\widetilde{\mathbf{n}}| \leq N}.$$

One has $CP = PC = 0$ and $P^t P = \widetilde{I}$.

Proposition 3.4. *The formal limit $\varepsilon \to 0$ of the singular Friedrichs system (17) is the non singular Friedrichs system*

$$\partial_t \widetilde{U} + \sum_{i=1}^{3} \partial_{x_i}\left(\widetilde{A}_i(\mathbf{x}, t)\widetilde{U}(\mathbf{x}, t)\right) = \widetilde{B}(\mathbf{x})\widetilde{U}(\mathbf{x}, t) \tag{36}$$

where $\widetilde{A}_i(\mathbf{x}) = P^t A_i(\mathbf{x})P$ for $1 \leq i \leq 3$ and $\widetilde{B}(\mathbf{x}) = P^t B(\mathbf{x})P$.

Proof. The solution of the full system (17) is written as a Hilbert expansion $U_\varepsilon = U_0 + \varepsilon U_1 + O(\varepsilon^2)$. Necessarily $U_0 \in \mathcal{K}$ son one can writes $U_0 = P\widetilde{U}$. Then multiplication all terms of the Friedrichs system by P^t on the left yields the claim. $\qquad \square$

The matrix P acts as a projection operator on the kernel $\mathcal{K}$, so the reduction model is also a projected model.

4 Models with electric field

We now reintroduce the electric field in the model (1). The electric field is self-consistent, that is it derives from the electric potential $\mathbf{E} = -\nabla\varphi$. Since one also has the Gauss law $\nabla \cdot \mathbf{E} = \rho_i(\mathbf{x}, t) - \rho_e$ where $\rho_e > 0$ is the reference constant electronic density (which is once again taken as constant in space for simplicity), one gets the Poisson equation

$$-\Delta\varphi = \int f dv - \rho_e. \tag{37}$$

The initial data is taken globally neutral that is

$$\rho_i - \rho_e = \int_x \left(\int_v f(\mathbf{x}, \mathbf{v}, 0) dv - \rho_e \right) dx = 0.$$

Then global neutrality is propagated by the transport equation, so one can write $\int_x \left(\int_v f(\mathbf{x}, \mathbf{v}, t) dv - \rho_e \right) dx = 0$ for all $t \geq 0$. To take into account the electric field in the moments models, one needs firstly to write the Poisson equation in function of the moments, and secondly to introduce the electric field in the Friedrichs systems. The next Lemma is dedicated to the first task.

Lemma 4.1. *The ion density is* $\rho_i = \int_v f^N(\mathbf{x}, \mathbf{v}, t) dv = \pi^{\frac{3}{4}} T^{\frac{3}{2}} u_{0,0,0}$.

Proof. With (7) and (14), one obtains

$$\psi^{(0,0,0)}(\mathbf{x}, \mathbf{v}) = e^{\frac{|\mathbf{v}|^2}{T}} \pi^{-\frac{1}{4}} e^{-|\mathbf{v}\cdot\mathbf{d}_0|^2} \pi^{-\frac{1}{4}} e^{-|\mathbf{v}\cdot\mathbf{d}_1|^2} \pi^{-\frac{1}{4}} e^{-|\mathbf{v}\cdot\mathbf{d}_2|^2} = \pi^{-\frac{3}{4}}.$$

The change of variable (15) yields $\int f dv = \pi^{\frac{3}{4}} T^{\frac{3}{2}} \int f \psi^{(0,0,0)} dw = \pi^{\frac{3}{4}} T^{\frac{3}{2}} u_{0,0,0}$.
□

The weak form of the moment model with an electric field writes as

$$\int_{\mathbf{v}} \left(\partial_t f^N + \mathbf{v} \cdot \nabla_x f^N + (\mathbf{E} + \frac{1}{\varepsilon} \mathbf{v} \times \mathbf{B}_0) \cdot \nabla_v f^N \right) \psi^{\mathbf{n}} dv = 0.$$

To discretize the terms proportional to $\mathbf{E}$, one defines three matrices $D^i(\mathbf{x}) = \left(d^i_{\mathbf{nm}}(\mathbf{x}) \right)_{|\mathbf{m}|, |\mathbf{n}| \leq N}$ with

$$d^i_{\mathbf{nm}}(\mathbf{x}) = \int_{\mathbf{v}} \partial_{v_i} \psi_{\mathbf{m}}(\mathbf{x}, \mathbf{v}) \psi^{\mathbf{n}}(\mathbf{x}, \mathbf{v}) dv, \qquad i = 1, 2, 3. \tag{38}$$

Lemma 4.2. *The coefficients of the matrices $D_i(\mathbf{x})$ are given by*

$$\begin{aligned}
d^i_{\mathbf{nm}}(\mathbf{x}) &= -T\mathbf{b}_0(x)_i \sqrt{2n_0} \delta_{m_0, n_0-1} \delta_{m_1, n_1} \delta_{m_2, n_2} \\
&\quad -T\mathbf{b}_1(x)_i \sqrt{2n_1} \delta_{m_0, n_0} \delta_{m_1, n_1-1} \delta_{m_2, n_2} \\
&\quad -T\mathbf{b}_2(x)_i \sqrt{2n_2} \delta_{m_0, n_0} \delta_{m_1, n_1} \delta_{m_2, n_2-1}.
\end{aligned} \tag{39}$$

14

Proof. One starts the analysis of (38) with an integration by parts $d_{\mathbf{nm}}^i(\mathbf{x}) = -\int_{\mathbf{v}} \boldsymbol{\psi}_{\mathbf{m}}(\mathbf{x},\mathbf{v})\partial_{v_i}\psi^{\mathbf{n}}(\mathbf{x},\mathbf{v})dv$, that is

$$d_{\mathbf{nm}}^i(\mathbf{x}) = -\int_{\mathbf{v}} \boldsymbol{\psi}_{\mathbf{m}}(\mathbf{x},\mathbf{v})\partial_{v_i}\left(\psi^{n_0}(\mathbf{v}\cdot\mathbf{d}_0(x))\psi^{n_1}(\mathbf{v}\cdot\mathbf{d}_1(x))\psi^{n_2}(\mathbf{v}\cdot\mathbf{d}_2(x))\right)dv.$$

One gets

$$\begin{aligned}
d_{\mathbf{nm}}^i(\mathbf{x}) = \quad & -\int_{\mathbf{v}} \boldsymbol{\psi}_{\mathbf{m}}(\mathbf{x},\mathbf{v})\mathbf{d}_0(x)_i(\psi^{n_0})'(\mathbf{v}\cdot\mathbf{d}_0(x))\psi^{n_1}(\mathbf{v}\cdot\mathbf{d}_1(x))\psi^{n_2}(\mathbf{v}\cdot\mathbf{d}_2(x))dv \\
& -\int_{\mathbf{v}} \boldsymbol{\psi}_{\mathbf{m}}(\mathbf{x},\mathbf{v})\mathbf{d}_1(x)_i\psi^{n_0}(\mathbf{v}\cdot\mathbf{d}_0(x))(\psi^{n_1})'(\mathbf{v}\cdot\mathbf{d}_1(x))\psi^{n_2}(\mathbf{v}\cdot\mathbf{d}_2(x))dv \\
& -\int_{\mathbf{v}} \boldsymbol{\psi}_{\mathbf{m}}(\mathbf{x},\mathbf{v})\mathbf{d}_2(x)_i\psi^{n_0}(\mathbf{v}\cdot\mathbf{d}_0(x))\psi^{n_1}(\mathbf{v}\cdot\mathbf{d}_1(x))(\psi^{n_2})'(\mathbf{v}\cdot\mathbf{d}_2(x))dv.
\end{aligned}$$

With Lemma 2.1, one obtains

$$\begin{aligned}
d_{\mathbf{nm}}^i(\mathbf{x}) = \quad & -T\int_{\mathbf{v}} \boldsymbol{\psi}_{\mathbf{m}}(\mathbf{x},\mathbf{v})\mathbf{b}_0(x)_i\sqrt{2n_0}\psi^{n_0-1}(w_0)\psi^{n_1}(w_1)\psi^{n_2}(w_2)dw \\
& -T\int_{\mathbf{v}} \boldsymbol{\psi}_{\mathbf{m}}(\mathbf{x},\mathbf{v})\mathbf{b}_1(x)_i\sqrt{2n_1}\psi^{n_0}(w_0)\psi^{n_1-1}(w_1)\psi^{n_2}(w_2)dw \\
& -T\int_{\mathbf{v}} \boldsymbol{\psi}_{\mathbf{m}}(\mathbf{x},\mathbf{v})\mathbf{b}_2(x)_i\sqrt{2n_2}\psi^{n_0}(w_0)\psi^{n_1}(w_1)\psi^{n_2-1}(w_2)dw.
\end{aligned}$$

The orthogonality of the Hermite functions yields the claim. $\qquad\square$

Let us decompose $\mathbf{E} = (E_1, E_2, E_3)$.

Proposition 4.3. *The moment model (17) with electric field writes*

$$T^{\frac{3}{2}}\partial_t U(\mathbf{x},t) + \sum_{i=1}^{3}\partial_{x_i}\left(A_i(\mathbf{x})U(\mathbf{x},t)\right) - B(\mathbf{x})U(\mathbf{x},t) \qquad (40)$$

$$+ \sum_{i=1}^{3}E_i(\mathbf{x},t)D_i(\mathbf{x})U = \frac{1}{\varepsilon}C(\mathbf{x})U(\mathbf{x},t).$$

The reduced version of the system writes

$$T^{\frac{3}{2}}\partial_t\widetilde{U} + \sum_{i=1}^{3}\partial_{x_i}\left(\widetilde{A}_i(\mathbf{x},t)\widetilde{U}(\mathbf{x},t)\right) - \widetilde{B}(\mathbf{x})\widetilde{U}(\mathbf{x},t) + \sum_{i=1}^{3}E_i(\mathbf{x},t)\widetilde{D}_i(\mathbf{x},t)\widetilde{U}(\mathbf{x},t) = 0.$$

$$(41)$$

where the matrices are $\widetilde{D}_i(\mathbf{x}) = \widetilde{A}_i(\mathbf{x}) = P^t D_i(\mathbf{x})P$. *Both models must be coupled with the Poisson equation and* $\mathbf{E} = -\nabla\varphi$.

Proof. This is evident for (41) since the electric contribution is additive. The projection method explained in the proof of Proposition 3.4 yields the reduced system (41). $\qquad\square$

5 Numerical method

The numerical method that we use to solve either (40) or (41) consists in a splitting strategy which follows the structure of this article. That is in a first step we solve (40) or (41), and in a second step we solve the Poisson equation and reintroduce the electric contribution. We explain the methods with the full system of moments (40). Mutatis mutandi, the same method is used for the reduced system (41).

5.1 Resolution with a splitting algorithm

5.1.1 First step

The first step corresponds to solving the system

$$T^{\frac{3}{2}}\partial_t U(\mathbf{x},t) + \sum_{i=1}^{3} \partial_{x_i}\left(A_i(\mathbf{x})U(\mathbf{x},t)\right) - B(\mathbf{x})U(\mathbf{x},t) - \frac{1}{\varepsilon}C(\mathbf{x})U(\mathbf{x},t) = 0$$

during one time step $[t_n, t_{n+1}]$. For all $n \geq 0$, we note $U(\mathbf{x})^n$ the numerical evaluation of the unknown vector at time step $t_n = n\Delta t$ and $\widehat{U}(\mathbf{x})^{n+1}$ denotes the prediction at the end of this phase. For the time discretization we consider a Cranck-Nicolson scheme

$$T^{\frac{3}{2}}\frac{\widehat{U}(\mathbf{x})^{n+1} - U(\mathbf{x})^n}{\Delta t} + \sum_{i=1}^{3} \partial_{x_i}\left(A_i(\mathbf{x})U(\mathbf{x})^{n+\frac{1}{2}}\right) - B(\mathbf{x})U(\mathbf{x})^{n+\frac{1}{2}}$$

$$-\frac{1}{\varepsilon}C(\mathbf{x})U(\mathbf{x})^{n+\frac{1}{2}} = 0$$

where $U(\mathbf{x})^{n+\frac{1}{2}} = \frac{\widehat{U}(\mathbf{x})^{n+1}+U(\mathbf{x})^n}{2}$. For the space discretization we consider a Finite Element method [18] with a Finite Element space $V_h \subset H^1(\Omega)$ which is very common in the discretization of incompressible flow [18]. For the full system of moments (40) we take

$$U(\mathbf{x})^n \in X_h := V_h^{\frac{(N+1)(N+2)(N+3)}{6}} \qquad \text{for all } n \geq 0. \tag{42}$$

One obtains the variational formulation for all test vectorial functions $V \in X_h$

$$
\begin{aligned}
T^{\frac{3}{2}} \int \frac{\widehat{U}(\mathbf{x})^{n+1}-U(\mathbf{x})^n}{\Delta t} \cdot V(\mathbf{x})dx \;=\;& \sum_{i=1}^{3} \int A_i(\mathbf{x})U(\mathbf{x},t)\cdot\partial_{x_i}V(\mathbf{x})dx \\
& + \int B(\mathbf{x})U(\mathbf{x})^{n+\frac{1}{2}}\cdot V(\mathbf{x})dx \\
& + \frac{1}{\varepsilon}\int C(\mathbf{x})U(\mathbf{x})^{n+\frac{1}{2}}\cdot V(\mathbf{x})dx.
\end{aligned}
\tag{43}
$$

To take into account the variation in space of the different matrices and vectors, the bilinear forms are assembled with numerical integration.

5.1.2 Second step

We solve the remaining part during the same time step $[t_n, t_{n+1}]$

$$T^{\frac{3}{2}}\partial_t U(\mathbf{x},t) + \sum_{i=1}^{3} E_i(\mathbf{x},t)D_i(\mathbf{x})U = 0. \tag{44}$$

Firstly we solve the Poisson equation, with a Finite Element Poisson solver. Then we calculate the electric field with $\mathbf{E} = -\nabla\varphi$. Finally we solve (44) with a Cranck-Nicolson method

$$T^{\frac{3}{2}}\frac{U(\mathbf{x})^{n+1} - \widehat{U}(\mathbf{x})^{n+1}}{\Delta t} + \sum_{i=1}^{3} E_i^n(\mathbf{x},t)D_i(\mathbf{x})\frac{U(\mathbf{x})^{n+1} + \widehat{U}(\mathbf{x})^{n+1}}{2} = 0. \tag{45}$$

Since the extra cost is marginal, we solve (45) in the variational sense, that is we assemble bilinear formulation with numerical quadratures

$$T^{\frac{3}{2}} \int \frac{U(\mathbf{x}_j)^{n+1} - \widehat{U}(\mathbf{x}_j)^{n+1}}{\Delta t} \cdot V(\mathbf{x})dx$$

$$+ \sum_{i=1}^{3} \int E_i^n(\mathbf{x}_j, t)D_i(\mathbf{x}_j)\frac{U(\mathbf{x}_j)^{n+1} + \widehat{U}(\mathbf{x}_j)^{n+1}}{2} \cdot V(\mathbf{x})dx = 0. \qquad (46)$$

5.2 Numerical implementation

To test the algorithmic structure of the anisotropic method of moments, we have developed a dedicated research code[1] written in C. We employ the finite element (FE) method for discretization in space, and finite differences for time discretization with an implicit procedure to reach unconditional numerical stability. At each time step the set of linear equations are solved with the Krylov method (e.g. GMRES method [34]), with initial guess given by the solution at the previous time step. In the following, we discuss the details of the numerical implementation.

5.2.1 Time discretization

We apply a finite difference (FD) method in time. First we need a mesh in time, here taken as uniform with mesh points

$$t_n = n\Delta t, \quad n = 0, 1, \ldots, N_{\text{end}}.$$

5.2.2 Space discretization

We are particularly interested in an effective numerical solution, so we assume a regular simplicial triangulation $\mathcal{T}_h(\Omega)$ of the domain Ω, and we assume $\overline{\Omega} = \cup_{\tau \in \mathcal{T}_h(\Omega)} \overline{\tau}$. We use standard notations and definitions for the Finite Element Method (FEM). We shall denote $V_h(\Omega) \subset H^1(\Omega)$ the space generated by conforming $\mathbb{P}_k$-Lagrange functions ($k \geq 1$) constructed on $\mathcal{T}_h(\Omega)$,

$$V_h(\Omega) := \{v_h \in C^0(\overline{\Omega}) : v_h|_\tau \in \mathbb{P}_k(\tau), \forall \tau \in \mathcal{T}_h(\Omega)\}.$$

A Galerkin method is naturally formulated where all functions and test functions in (43) nd (46) are taken in X_h (42).

5.3 Numerical results

In this section, we test the discrete moment method by discussing standard test problems of the literature. The first three tests are designed to validate the pure transport equation, and the reduced gyro-kinetic model. Next, we consider

---

[1]Repository: `https://gitlab.lpma.math.upmc.fr/muffin/muf`.

cases with the Landau damping test and the Bernstein-Landau paradox. The simulations presented in this work are carried on a Dell XPS with processor i7-6700HQ. The open source Gmsh [17] has been used for mesh generation and post-processing.

5.3.1 The transport equation

Consider the Vlasov equation (1). If we suppose that the magnetic field vanishes (e.g. $\varepsilon \to +\infty$) at any time and any position, we obtain the x-transport equation

$$\partial_t f + \mathbf{v} \cdot \nabla_x f = 0. \tag{47}$$

The domain is an unit cube $\Omega = L_x \times L_y \times L_z = [0,1]^3$ with spatial periodic boundary conditions. We take $\varepsilon = 10^{15}$ so the magnetic field is eliminated. An initial condition is given as follows:

$$\begin{cases} u_{\mathbf{m}}(t=0,\mathbf{x}) = 1 + \cos(2\pi(x_1 + x_2 + x_3)), & \mathbf{m} = (0,0,0), \\ u_{\mathbf{m}}(t=0,\mathbf{x}) = 0, & \mathbf{m} \neq (0,0,0). \end{cases}$$

An analytical solution of (47) is $f(t,x,v) = \pi^{\frac{3}{4}} \exp^{-|v|^2/2}(1 + \sum_{i=1}^{3} \cos(2\pi(x_i - v_i t)))$. One deduces a reference/analytical solution for the first moment

$$u_{0,0,0}^{\text{ana}}(t,\mathbf{x}) = 1 + \cos(2\pi(x_1 + x_2 + x_3))\exp^{-3\pi^2 t^2}.$$

The numerical solution is computed using a standard first-order nodal FE method on a mesh made of hexahedra and generated with Gmsh [17]. The following numerical setting has been considered: P1 finite elements with 7 points of discretization in each spatial direction and mesh made of 343 nodes, 216 P1 hexahedra. The linear system resulting from the FE discretization is solved using GMRES [34]. For the velocity space, we take $N = 10$ that is 286 moments.

First test case

It is the transport equation (47) with a constant basis $\mathbf{b}_0(\mathbf{x}) = \{1,0,0\}^\top$. The results are given on Figure 3. We compare the numerical solution of the x-transport equation and the exact solution. We observe that the numerical solution is a good approximation to the exact solution when $t \leq 0.5$s. For later time there is a divergence which is classical for the discretization of such kinetic equations. As explained in [29], the numerical scheme exhibits an artificial recurrence effect because the model converges the energy over a finite number of modes. The continuous model also preserves a similar energy but over an infinite number of modes. It is visible on Figure 3 where the first moment starts to build up again for $t \geq 0.5$s.
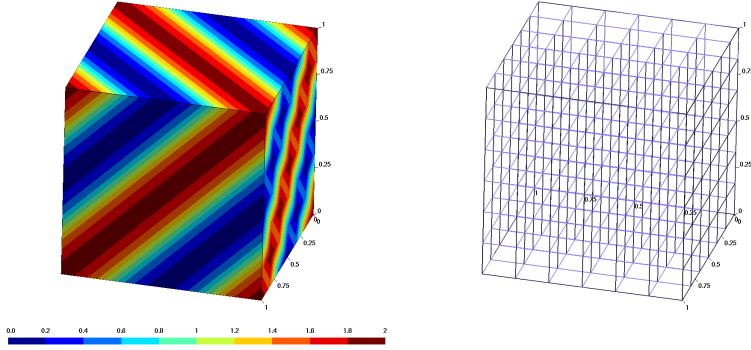
18

Figure 2: $x-$transport equation. (left) initial condition of $u_{0,0,0}(0, \mathbf{x})$. (right) mesh.
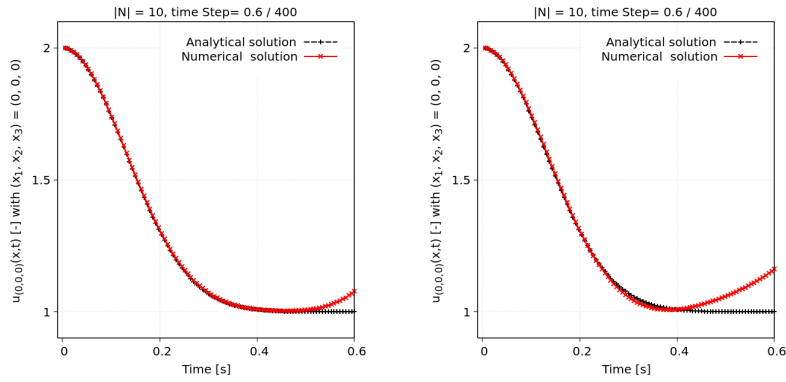

Figure 3: $x-$transport equation. (left) numerical solution of $u_{0,0,0}(t, \mathbf{x})$ for the case with a constant basis. (right) numerical solution of $u_{0,0,0}(t, \mathbf{x})$ for the case with a non-constant basis. $\mathbf{x} = (0, 0, 0)$.

Second test case

It is the transport equation (47) with a non-constant basis

$$\mathbf{b}_0(\mathbf{x}) = \{0, \cos(2\pi x_3), \sin(2\pi x_3)\}^\top.$$

Figure 3 shows the analytical solution and numerical solution. It shows that the numerical solution is a good approximation to the exact solution when $t < 0.4s$, still before the time of the artificial recurrence phenomenon.
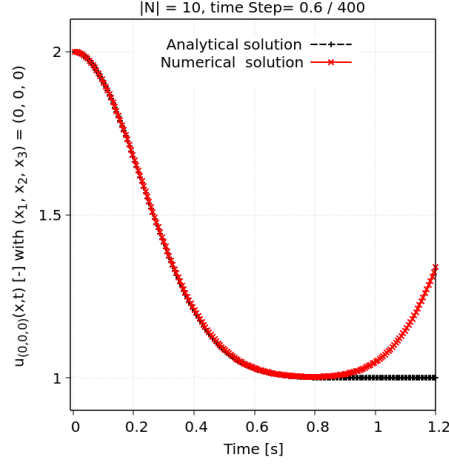
Figure 4: Gyro model. Numerical solution of $u_{0,0,0}(t, \mathbf{x})$.

Third test case with reduced gyro-kinetic model

Now the magnetic field is non zero $\mathbf{B}_0(\mathbf{x}) = \mathbf{b}_0(\mathbf{x})\{1, 0, 0\}^\top$ in the simplified equation

$$\partial_t f_\epsilon + \mathbf{v} \cdot \nabla_x f_\epsilon + \frac{1}{\varepsilon} \mathbf{v} \times \mathbf{B}_0(\mathbf{x}) \cdot \nabla_v f_\epsilon = 0. \tag{48}$$

One can find an equivalence principle where $f(t, \mathbf{x}, \mathbf{v}) = g(t, \mathbf{x}, v_1, \mu)$ for all t, $\mathbf{x}$, v_1 and μ where $\mu = \sqrt{v_2^2 + v_3^3}$. Provided that g is the solution to

$$\partial_t g + v_1 \partial_{x_1} g = 0, \tag{49}$$

with initial condition $g(0, \mathbf{x}, v_1, \mu) = \exp^{-|v^2|/2}(1 + \cos 2\pi x_1)$, then it can be shown that f is the exact solution of the magnetized transport. It means that f is equal to its gyroaverage g. Since

$$g(t, \mathbf{x}, v_1, \mu) = \exp^{-|v^2|/2}(1 + \cos 2\pi x_1 \exp^{-\pi^2 t^2})$$

one easily calculates the moment $\mathbf{u}_{(0,0,0)}(\mathbf{x}, t)$.

For numerical simulation we use the reduce method where $\widetilde{N} = 36$ is the reduced number of moments. The other physical and numerical configurations are the same as in the previous cases. Figure 4 compares the analytical solution and the numerical solution. Once again the numerical solution is a good approximation to the exact solution before the time of the artificial numerical recurrence $t \approx 0.8$.

5.3.2   Linear Landau damping

We perform a convergence study on the Landau damping problem. Landau damping is a standard test for collisionless plasmas, which is the effect of damping of longitudinal space charge waves. It occurs because of the energy exchange

between a wave initially excited in the plasma and particles in the plasma that are resonant with it. We consider the non-linear Vlasov-Poisson system:

$$\begin{cases} \partial_t f + \mathbf{v} \cdot \nabla_x f + \left(\mathbf{E} + \frac{1}{\varepsilon} \mathbf{v} \times \mathbf{B}_0(\mathbf{x}) \right) \cdot \nabla_v f = 0, \\ \nabla \cdot \mathbf{E} = \int f \, dv - \rho_e. \end{cases}$$

We keep periodic solutions in x_1-direction, and consider the initial density function

$$f(0, \mathbf{x}, \mathbf{v}) = \left(\frac{1}{\sqrt{2\pi}} \right)^3 (1 + \alpha \cos(kx_1)) \exp^{-|\mathbf{v}|^2/2}.$$

We seek a solution of the form,

$$f(t, \mathbf{x}, \mathbf{v}) = f_1(t, x_1, v_1) \left(\frac{1}{\sqrt{2\pi}} \exp^{-v_2^2/2} \right) \left(\frac{1}{\sqrt{2\pi}} \exp^{-v_3^2/2} \right),$$

where $f(t, \mathbf{x}, \mathbf{v})$ satisfies the non-linear Vlasov equation and the initial condition if and only if $f_1(t, x_1, v_1)$ is a solution of the follwing Vlasov-Poisson in one dimension in space x_1 and velocity v_1,

$$\begin{cases} \partial_t f + v_1 \partial_{x_1} f + E_1 \partial_{v_1} f = 0, \\ \partial_{x_1} E_1 = \int f \, dv - \rho_e. \end{cases}$$

initialized with

$$f(0, \mathbf{x}, \mathbf{v}) = \frac{1}{\sqrt{2\pi}} (1 + \alpha \cos(kx_1)) \exp^{-v_1^2/2}.$$

The approximate solution to the system above is given in page 58 of [36]. Moreover, we can compute an approximate $E_1(t, x_1)$ using the moment method based on the splitting strategy in this work and compare to the approximate solution

$$E_1(x_1, t) \approx 4\alpha \times 0.424666 \exp^{-0.0661t} \sin(0.4x_1) \cos(1.2850t - 0.1157725).$$

We choose the values $\alpha = 0.001$ and $k = 0.4$ in the second line of the table in page 58 of [36]. This is a good approximate solution of the exact solution for large times, which is also used as a test case in [5, 33].

We take the charge of the ions equal to one, and only consider $u_\mathbf{m}$ with respect to the velocity variable v_1 and v_2. The domain is a rectangular cuboid $\Omega = L_x \times L_y \times L_z = [0, 2\pi/k] \times [0, 1]^2$. We take $\varepsilon = 10^{15}$ so that the magnetic field vanishes. The numerical setting is considered as follows: P1 finite elements with 127 points of discretization in x_1-direction, and 3 points of discretization in x_2-direction and x_3-direction. The mesh of this setting is made of 1143 nodes, 504 P1 hexahedra. For velocity space, $N = 100$ that is 5151 moments. In Figure 5, we plot the electric energy, and we can see that the numerical solution is reasonably accurate.
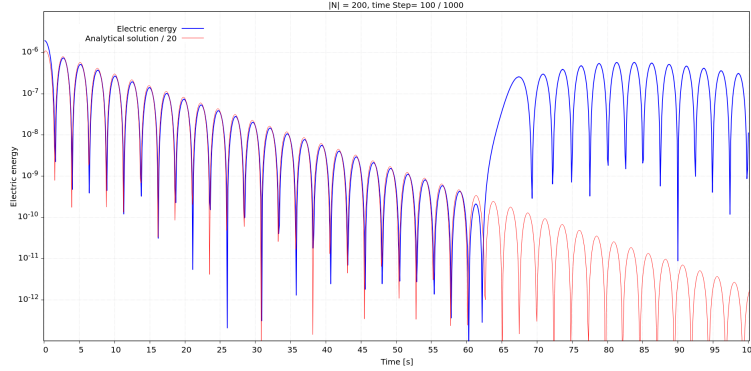
Figure 5: Landau damping. Damped electric field with $k = 0.4$, and $\varepsilon = 10^{15}$.

5.3.3 The Bernstein-Landau paradox

The next test case that we study is the Bernstein-Landau paradox in an electrostatic plasma, whereby electric field and charge density fluctuations have time oscillatory behavior in the presence of a magnetic field. Magnetized plasmas can prevent Landau damping, which was demonstrated by Bernstein [2] that in the presence of a constant magnetic field, the electric field does not decay for a long time, and in fact has a time-varying oscillatory behavior.

The physical and numerical configuration is the same with the Landau damping test, despite that $\varepsilon = 10$. It shows that the damping is replaced by a recurrence phenomenon of period $T_c = 2\pi\varepsilon$ when there is a magnetic field. This recurrence is a consequence of the series based on the eigenvectors expansion in the regime of non zero magnetic field [33, 5]. In Figure 6, we plot the electric en-
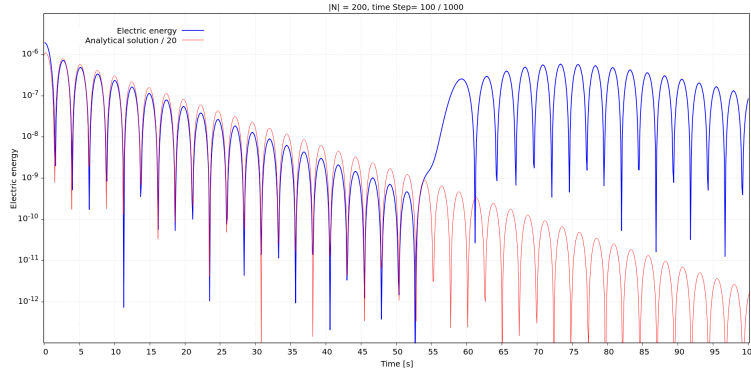

Figure 6: Bernstein-Landau paradox. Undamped electric field with $k = 0.4$, and $\varepsilon = 10$.

ergy for Bernstein-Landau paradox test case, and we can observe that recurrence

22

is visible with the period $2\pi\epsilon$. In other words, the Bernstein-Landau paradox is an entirely "physical" phenomenon arising from the non-zero magnetic field [33, 5].

5.3.4   Diocotron

The chosen initial data is inspired by [10, 6]. It is a Maxwellian in velocity and a ring-shape distribution in space with a perturbation in angle

$$
f_0(\mathbf{x}, \mathbf{v}) = \begin{cases} \dfrac{n_0}{(\sqrt{2\pi})^3}(1 + \eta\cos(k\theta)) \exp^{-4(r-6.5)^2} \exp^{-|\mathbf{v}|^2/2}, & r^- \leq r \leq r^+, \\ 0, & \text{otherwise,} \end{cases}
\tag{50}
$$

where $\mathbf{x} = (x_1, x_2, x_3)$, $\mathbf{v} = (v_1, v_2, v_3)$, $r = \sqrt{x_2^2 + x_3^2}$. Correspondingly, the initial moment is given as follows:

$$
u_{0,0,0} = \begin{cases} (2^{-3/2}\pi^{-3/4}) n_0 (1 + \eta\cos(k\theta)) \exp^{-4(r-6.5)^2}, & r^- \leq r \leq r^+. \\ 0, & \text{otherwise,} \end{cases}
\tag{51}
$$

The non-homogenous magnetic field is taken as

$$
\mathbf{B}_0(\mathbf{x}) = \omega_c(\mathbf{x}) \frac{1}{\sqrt{1 + \alpha^2 x_3^2 + \alpha^2 x_2^2}}(1, \alpha x_2, -\alpha x_3)^\top.
$$

The spatial domain is a cartesian geometry $\mathbf{x} = (x_1, x_2, x_3) \in \Omega = [0, 1] \times [-13, +13] \times [-13, +13]$. We choose $n_0 = 1$, $\eta = 0.01$, $k = 4$ $r^- = 5$, $r^+ = 8$ and discretize the spatial domain Ω with $N_{x_1} = 2$ and $N_{x_2} = N_{x_3} = 64$ points. As a diagnostic, we consider the density $\int_{\mathbb{R}^3} u_{0,0,0}(t, \mathbf{x})\psi_{0,0,0}(\mathbf{x}, \mathbf{v})d\mathbf{v} = 2^{3/2}\pi^{3/4} u_{0,0,0}(t, \mathbf{x})$. The results are displayed in Figure 7.

One observes that the ring is transformed at a later in a square, as in [6]. The calculation for later time is possible with our numerical tool, but so far the results are delicate to interpret so far to postpone the presentation of such more physical results.

5.4   Comments on the numerical cost of the simulations

Even with this important numerical cost, we foresee two situations where our discretization strategy with anistropic moments is worth the game. The first is to use the reduced model as a way to drastically diminish the number of moments. The second one is to use our methodology to discretize kinetic equations for electrons, where the small mass of the electron is known to hamper the time step for explicit Euler discrete methods. Our implicit solver is indeed a natural option to bypass the cost of explicit computations in such situations.

The dedicated research code[2] (written in C) uses state of the art compressing techniques for manipulations of sparse matrices. However the numerical solver

---

[2]Repository: `https://gitlab.lpma.math.upmc.fr/muffin/muf`.

(a) $t = 0.1$ **(b)** $t = 1.0$

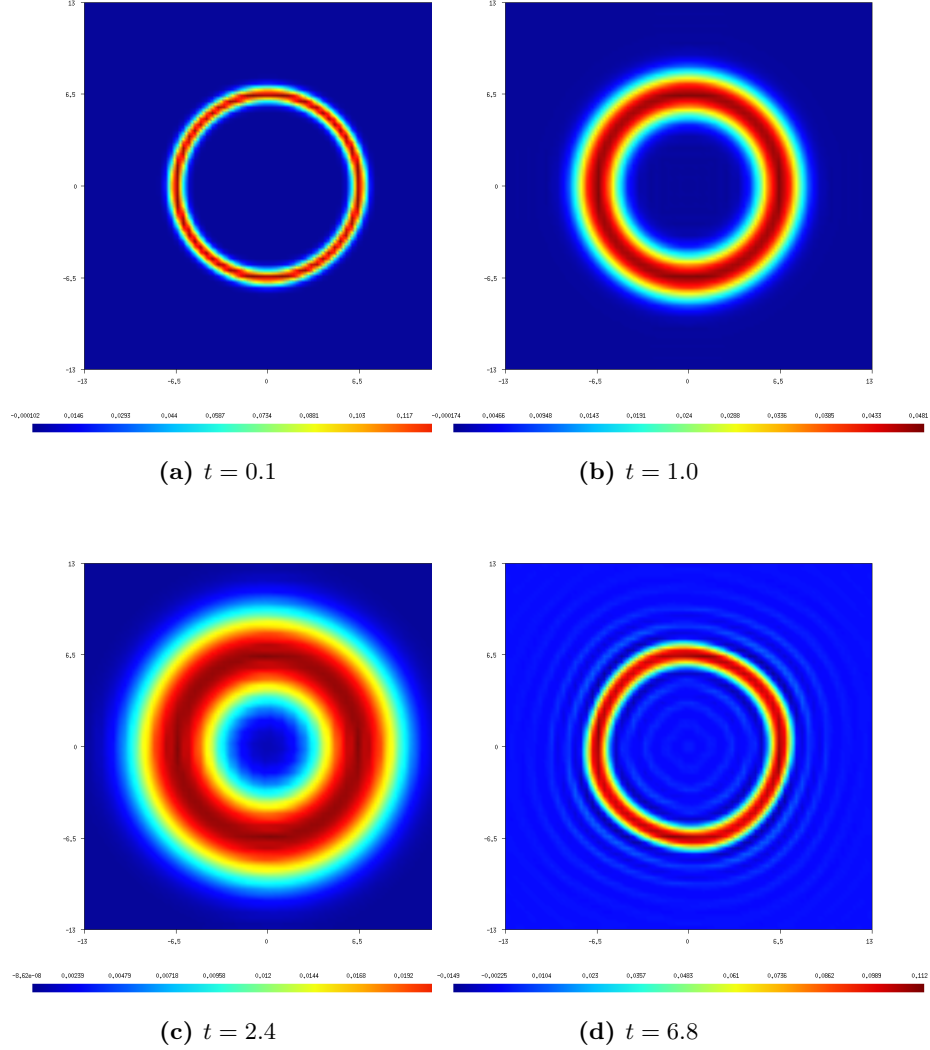**(c)** $t = 2.4$ **(d)** $t = 6.8$

Figure 7: The full 3D Vlasov-Poisson system. Numerical solution of $u_{0,0,0}(t, \mathbf{x})$ with initial condition (51) with $\alpha = 0$. The $|N|$ for the moment method is equal to 70.

used to solve the implicit Euler system has its own cost, which is multiplied by the number of time steps required to reach the final time. We are currently working on the optimization of this numerical tool in order to minimize the time of simulation. It will require to develop acceleration techniques and to use the ressources of HPC (High Performing Computing).

A Proof of formula (34)

The proof comes from (6). One has

$$
\begin{aligned}
F_s(w_2, w_3) &= \frac{1}{2^{2s}s!\sqrt{\pi}}e^{\frac{w_2^2+w_3^2}{2}}\sum_{r=0}^s \frac{s!}{r!(s-r)!}\frac{d^{2r}}{dw_2^{2r}}e^{-w_2^2}\frac{d^{2(s-r)}}{dw_2^{2(s-r)}}e^{-w_3^2} \\
&= \frac{1}{2^{2s}s!\sqrt{\pi}}e^{\frac{w_2^2+w_3^2}{2}}\left(\partial_{w_2}^2 + \partial_{w_3}^2\right)^s e^{-(w_2^2+w_3^2)}.
\end{aligned} \tag{52}
$$

This formula shows by recurrence that $F_s(w_2, w_3) = p_s(w_2^2 + w_3^2)e^{-\frac{w_2^2+w_3^2}{2}}$ where p_s is some real polynomial of degree less or equal to s. Integrations by parts show that $\int\int F_s(w_2, w_3)F_{s'}(w_2, w_3)dw_2 dw_3 = 0$, where $s \neq s'$. It can be written in radial coordinates $(w = \sqrt{w_2^2 + w_3^2})$ as $\int_0^\infty p_s(w)p_{s'}(w)e^{-w}dw = 0$ $s \neq s'$. We note the Rodrigues type formula

$$
p_s(w^2) = e^{w^2}\left(\frac{d^2}{dw^2} + \frac{1}{w}\frac{d}{dw}\right)^s e^{-w^2}. \tag{53}
$$

This compact formula seems original with respect to the classical literature [31]. It is easy to reduce it to the classical formula for Laguerre polynomials.

Let us make a change of variable $x = w^2 \in \mathbb{R}^+$. One checks the identity $\frac{d^2}{dw^2} + \frac{1}{w}\frac{d}{dw} = 4\left(x\frac{d^2}{dx^2} + \frac{d}{dx}\right)$. So $p_{s+1}(x) = 4e^x\left(x\frac{d^2}{dx^2} + \frac{d}{dx}\right)^{s+1}e^{-x} = 4e^x\left(x\frac{d^2}{dx^2} + \frac{d}{dx}\right)(p_s(x)e^{-x})$. One obtains the iteration

$$
\begin{cases}
p_0(x) = 1, \\
p_{s+1}(x) = 4\left(xp_s''(x) + (1 - 2x)p_s'(x) + (x - 1)p_s(x)\right).
\end{cases} \tag{54}
$$

Similar iteration formulas are known for Laguerre polynomials $(L_n(x))_{n\in\mathbb{N}}$, see [31]. In particular it is known that

$$
\begin{cases}
xL_n''(x) + (1 - x)L_n'(x) + nL_n(x) = 0, \\
(n + 1)L_{n+1}(x) - (2n + 1 - x)L_n(x) + nL_{n-1}(x) = 0, \\
xL_n'(x) - nL_n(x) + nL_{n-1}(x) = 0.
\end{cases}
$$

Elimination of $L_{n-1}(x)$ by subtraction of the last identity to the second one yields $(n + 1)L_{n+1}(x) - xL_n'(x) + (x - n - 1)L_n(x) = 0/$ Addition of the first identity yields $(n + 1)L_{n+1}(x) + xL_n''(x) + (1 - 2x)L_n'(x) + (x - 1)L_n(x) = 0$. Comparison with the iteration formula in (54) yields $p_n(x) = (-1)^n 4^n n! L_n(x)$.

References

[1] Antonsen,T.M. and Lane,B., Kinetic equations for low frequency instabilities in inhomogeneous plasmas. Phys. Fluids 23, 1205-1214 (1980).

[2] I. B. Bernstein. Waves in a plasma in a magnetic field. Physical Review, 109(1):10, 1958.

[3] Bottino A., Tran T.M., Sauter O., Vaclavik J. and Villard L., Linear gyrokinetic simulations using particles for small perpendicular wavelength perturbations. In: Theory of Fusion Plasmas, Proceedings of the International Workshop, Varenna, 2000, Compositori, Bologna, pp. 327-332 (2001)

[4] Brizard, A.J. and Hahm, T.S., Foundations of non linear gyrokinetic theory, Rev. Modern Phys. 79, 421-468 (2007).

[5] F. Charles, B. Després, A. Rege, and R. Weder. The magnetized vlasov–ampère system and the bernstein–landau paradox. Journal of Statistical Physics, 183(2):1–57, 2021.

[6] P. Chartier, N. Crouseilles, M. Lemou, F. Méhats, X. Zhao. Uniformly accurate methods for three dimensional Vlasov equations under strong magnetic field with varying direction. SIAM Journal on Scientific Computing, Society for Industrial and Applied Mathematics, 2020, 42 (2), pp.B520-B547.

[7] P. Degond and F. Filbet, On the Asymptotic Limit of the Three Dimensional Vlasov-Poisson System for Large Magnetic Field: Formal Derivation, Stat Phys 165:765-784, 2016.

[8] G. L. Delzanno, Multi-dimensional, fully-implicit, spectral method for the Vlasov-Maxwell equations with exact conservation laws in discrete form. J. Comp. Physics. 301, 338-356, 2015.

[9] B. Després. Symmetrization of Vlasov-Poisson equations. SIAM Journal on Mathematical Analysis, Society for Industrial and Applied Mathematics, 2014, 46 (4), pp.2554-2580.

[10] F. Filbet, L. M. Miguel Rodrigues. Asymptotically stable particle-in-cell methods for the Vlasov-Poisson system with a strong external magnetic field. SIAM Journal on Numerical Analysis, Society for Industrial and Applied Mathematics, 2016, 54 (2), pp.1120-1146.

[11] F. Filbet and M. Bessemoulin-Chatard, On the stability of conservative discontinuous Galerkin/Hermite spectral methods for the Vlasov-Poisson system, J. Comput. Phys. 451 (2022).

[12] F. Filbet and T. Xiong, Conservative discontinuous Galerkin/Hermite Spectral Method for the Vlasov-Poisson System, Commun. Appl. Math. Comput. 4 (2022).

[13] F. Filbet and T. Xiong, A Hybrid Discontinuous Galerkin Scheme for Multiscale Kinetic Equations, J. Comput. Physics, 372 (2018), pp. 841-863.

[14] F. Filbet and L.M. Rodrigues, Asymptotics of the three dimensional Vlasov equation in the large magnetic field limit, Journal de l'Ecole Polytechnique, Vol. 7 (2020), p. 1009-1067

[15] Frénod, E. and Sonnendrücker,E., Homogenization of the Vlasov equation and of the Vlasov-Poisson system with a strong external magnetic field. Asymptot. Anal. 18, 193-213 (1998)

[16] Frénod,E. and Sonnendrücker,E., Long time behavior of the two-dimensional Vlasov equation with a strong external magnetic field. Math. Models Methods Appl. Sci. 10, 539-553 (2000)

[17] C. Geuzaine and J.-F. Remacle. Gmsh: A 3-d finite element mesh generator with built-in pre-and post-processing facilities. International journal for numerical methods in engineering, 79(11):1309–1331, 2009.

[18] Roland Glowinski, Finite element methods for incompressible viscous flow, Handbook of Numerical Analysis Volume 9, 3-1176, 2003.

[19] Golse, F. and Saint-Raymond, L., The Vlasov-Poisson system with strong magnetic field. J. Math. Pures Appl. 78, 791-817 (1999).

[20] V. Grandgirard, J. Abiteboul, J. Bigot, T. Cartier-Michaud, N. Crouseilles, et al.. A 5D gyrokinetic full-f global semi-lagrangian code for flux-driven ion turbulence simulations. Computer Physics Communications, Elsevier, 2016, 207, pp.35-68.

[21] Hauray, M. and Nouri, A., Well-posedness of a diffusive gyro-kinetic model. Ann. Inst. H. Poincaré Anal. Non Linéaire 28, 529-550 (2011).

[22] Hazeltine, R.D. and Ware, A.A., The drift kinetic equation for toroidal plasmas with large mass velocities. Plasma Phys. 20, 673-678 (1978).

[23] J. P. Holloway, Spectral velocity discretizations for the Vlasov-Maxwell equations, Transport Theory and Statistical Physics, 25:1, 1-32, 1996.

[24] Kim, C.C. and Parker, S.E., Massively parallel three dimensional toroidal gyrokinetic flux-tube turbulence simulations. J. Comput. Phys. 161, 589-604 (2000)

[25] J. Madsen, Full-F gyrofluid model, Physics of Plasmas (1994-present) 20, 072301, 2013.

[26] N. R. Mandell, W. Dorland, M. Landreman, Laguerre-Hermite Pseudo-Spectral Velocity Formulation of Gyrokinetics, Journal of Plasma Physics, Volume 84, Issue 1, 2018.

[27] G. Manzini, G. L. Delzanno, J. Vencels, and S. Markidis. A Legendre-Fourier spectral method with exact conservation laws for the vlasov–poisson system. Journal of Computational Physics, 317:82–107, 2016.

[28] G. Manzini, G. L. Delzanno, J. Vencels and S. Markidis, A Legendre-Fourier spectral method with exact conservation laws for the Vlasov-Poisson system, J. Comput. Phys. 317, 82-107, 2016.

[29] M. Mehrenberger, L. Navoret, N. Pham, Recurrence phenomenon for Vlasov-Poisson simulations on regular finite element mesh, Communications in Computational Physics, Commun. Comput. Phys., 28 (2020), pp. 877-901.

[30] Miyamoto, K., Plasma Physics and Controlled Nuclear Fusion, vol.38, Springer, Berlin (2006).

[31] Olver, Frank & Lozier, Daniel & Boisvert, Ronald & Clark, Charles. (2010). NIST Handbook of Mathematical Functions.

[32] S. Possaner, Gyrokinetics from variational averaging: Existence and error bounds J. Math. Phys. 59, 082702 (2018); `https://doi.org/10.1063/1.5018354`

[33] A. Rege. Kinetic models for magnetized plasmas. PhD thesis, Sorbonne Université, 2021.

[34] Y. Saad and M. H. Schultz. Gmres: A generalized minimal residual algorithm for solving nonsymmetric linear systems. SIAM Journal on scientific and statistical computing, 7(3):856–869, 1986.

[35] J. W. Schumer and J. P. Holloway. Vlasov simulations using velocity-scaled hermite representations. Journal of Computational Physics, 144(2):626–661, 1998.

[36] E. Sonnendrücker. Modèles cinétiques pour la fusion. Master notes, 2:11, 2008.